BIFURCATION ANALYSIS OF A NONLOCAL TWO-COMMUNICATION MECHANISM MODEL FOR ANIMAL AGGREGATION WITH **O(2)**-SYMMETRY

By

Alberto Quintin N. Alinas

A Thesis Submitted in Partial Fulfillment

of the Requirements for the Degree of

Master of Science

in

The Faculty of Science

Modelling and Computational Science

December 19, 2016

Abstract

The study of animal aggregations has become a topic of great interest due to its practical applications and theoretical significance. The common occurrence of these aggregations in nature lead to a large variety of models that have been proposed and investigated over the years. In this thesis, we present a class of models that considers communication among the individuals to be the basis of the social interaction within a group. In particular, we present the nonlocal hyperbolic model with two-communication mechanisms in a domain with periodic boundary conditions introduced by Eftimie (*J. Theoretical Biol.*, **337**, 42-53, 2013). We show that the system is symmetric with respect to the group $\mathbf{O(2)}$ of spatial translations and reflection. Using symmetry techniques from the text by Golubitsky et al. (Singularities and Groups in Bifurcation Theory, Vol II. Springer, 1988), we focus on studying a spatially homogeneous equilibrium and its linear stability as a function of parameters for attraction and repulsion. Given this symmetry perspective, we obtain a decomposition of the linearization at the equilibrium in terms of 4×4 matrices. We obtain a diagram in the attraction and repulsion parameter space for which the critical curves forming the boundary of the asymptotic stability region for the equilibrium are shown. Given the obtained boundaries, we then describe the patterns obtained via steady-state and Hopf bifurcations with symmetry as critical curves are crossed.

Acknowledgements

I would like to express my gratitude to my supervisor Dr. Pietro-Luciano Buono. He gave me the opportunity to pursue a post-graduate degree which I did not think I would ever do. His patience with me throughout my program has helped me maintain my passion, drive and focus in completing my degree. I would also like to thank my examining committee members, Dr. Lennaert van Veen, Dr. Sean Bohun and Dr. Hendrick de Haan for their words of encouragement, valuable input and suggestions.

Many thanks to the faculty and staff of the Modelling and Computational Science department, especially to my colleagues from the CLAIM Lab, our discussions and interactions have been an important part of my graduate studies. I would like to thank my friend Jamil Jabbour for encouraging me to pursue graduate studies and continually guiding me throughout my program. I would also like to thank Nicholas Faulkner for his guidance, our discussions about group-representation theory have been an important part of my learning process.

A special thanks to the Tecson family for supporting my family and I during our early years in Canada. Your hospitality during those years has helped me complete my undergraduate degree for which I am eternally grateful.

I would like to thank my parents Arthur and Hermila Alins for supporting me emotionally and financially throughout this endeavour. Your support has allowed me to complete this program in a comfortable and enjoyable manner for which I am forever thankful.

Finally, to my wife Karen, thank you for providing me the inspiration and motivation during the times when I feel like I cannot continue to study anymore. It has been a tough two and a half years but we did it! The completion of this thesis would be impossible without your love and support.

Para Sa Mga Tinatamad Mag-aral

Author's Declaration

I declare that this work was carried out in accordance with the regulations of the University of Ontario Institute of Technology. The work is original except where indicated by special reference in the text and no part of this document has been submitted for any other degree. Any views expressed in the dissertation are those of the author and in no way represent those of the University of Ontario Institute of Technology. This document has not been presented to any other University for examination either in Canada or overseas.

Alberto Quintin N. Alinas

Date: December 19, 2016

Contents

List of Tables

List of Figures

Chapter 1

Introduction

In nature, animals are often observed to form groups (Figs. 1.1a–1.1h), operationally these animal aggregations fit into two classes; *self-organizing* aggregations or aggregations that form in response to internal cues, and aggregations that form in response to external cues such as light or food [12, 30]. Due to the common occurrence of self-organizing grouping behaviour in nature (e.g., schools of fish, flocks of birds, swarms of insects, herds of ungulates, etc.) many studies on the reasons behind these behaviours have been conducted and are fairly well understood. Classically, aggregations have been viewed as an evolutionary advantageous state that allow individuals to improve their abilities to overcome the challenges presented by their environment [24, 30] such as; gaining foraging efficiency and anti-predator benefits, conservation of energy, mating strategy, etc. The concept of *group defense* as described by Freedman and Wolkowicz [15], is the phenomenon where predation is decreased or prevented altogether due to the increased ability of the prey to better defend themselves when their number is large enough [16]. Several studies show that size relations between predator and prey play an important role behind group formation [29] (e.g., Antarctic krill forming a group (Fig. 1.1b) for protection against predators [33], a troop of monkeys engaging in cooperative defense behaviours [29], a herd of oxen being able to orient themselves in a position to defend (Fig. 1.1g) against attacks by predators [15], etc.).

Group formation for energy conservation has also been documented by various studies, for example, Ritz [33] discusses how aggregation of aquatic crustaceans is a strategy that optimises energy expenditure and maximise food capture. The often observed *V-shaped* flight orientation in fowls (Fig. 1.1e) are documented by various studies, it has been shown that this self organizing behaviour leads to conservation of energy during flight. Cutts and Speakman [7] discusses this behaviour for skeins of pink-footed geese and Weimerskirch et al. [38] provides empirical evidence that formation flight of great white pelicans provides a significant aerodynamic advantage over solo flight; there, it is shown that group formation during flight reduces their energy expenditure while flying at a similar speed. Group formation to conserve energy is also seen in southern flying squirrels [34], the formation of large winter nest aggregations allow the squirrels to raise tree cavity temperatures and reduce individual heat loss. Spatial aggregation also influences reproduction in animal populations, it is shown in [8] that the unionid mussel *Elliptio complanata* takes advantage of spatial aggregation in order to find mates and reproduce in a more successful manner. Pattern formation is not only beneficial to animal survival mechanisms, but also in human activities. In particular, Lukes et al. [26] discusses the effect of *drafting* on cyclists (Fig. 1.1h); there, it is observed that cyclists riding in groups will orient themselves in a drafting formation or paceline to reduce the effort required to maintain a specific speed. Due to the large amount of research on the formation of animal aggregations, in particular the complex patterns and characteristic dynamics that arise from these studies. Spatial and spatiotemporal pattern formations in animal aggregations have become a topic of great interest due to its theoretical significance and practical applications [4, 10, 11, 12, 13, 20, 22, 25, 31], and references therein. Displaying a strong resemblance to fluid flow, animal aggregation models can be represented as being either being either *Lagrangian* (individual-based models) or *Eulerian* (continuum models) [12, 14, 30]. The first classification of models is based on the rules that governs the movements of individuals with Lagrangian equations of motion [12, 30]. Numerical simulations show that Lagrangian models may exhibit group patterns such as,

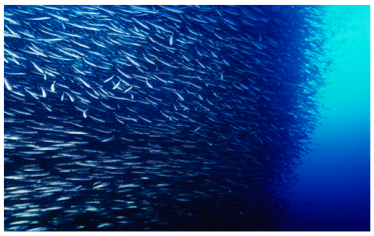

(a) School of fish

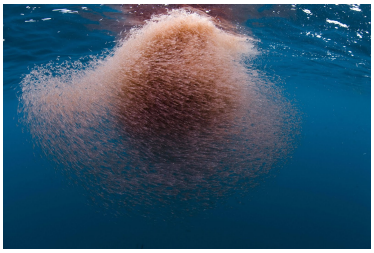

(b) Swarm of krill

(c) Starling murmuration

(d) Pack of wolves isolating a bison

(e) A flock of white pelicans in a V-formation

(f) Swarm of locusts in resting position

(g) Muskoxen herd in a defensive position

(h) Cyclists in a paceline

Figure 1.1: Images of different animal aggregations

swarms, tori, polarized groups, parallel groups etc., [6, 13], the simulations also demonstrate a very close resemblance of the group structures it generated from the structures observed in nature [6, 12, 37], and references therein. Lagrangian models are mostly applied to small groups of organisms [6, 12, 13, 23], due to the lack of analytical techniques and computational difficulties [11] within the models. On the other hand, Eulerian models are used to study the dynamics of the density of the individuals in the group. Based on a diffusion approximation of random motion [9, 30] these models are usually described by partial differential equations and thus allow one to use well-established analytical techniques to investigate the mechanisms behind the patterns in much bigger groups [12, 13, 18, 19]. Continuum models can be classified as *parabolic* or *hyperbolic* [10, 12, 13], both types of models may consider the social interactions (e.g., repulsion, attraction, alignment) between neighbouring individuals to be *local* (i.e., immediate neighbours or local effects of the environment are considered to be important), or *nonlocal* (i.e., distant individuals from a reference individual or the nonlocal effects of the environment are considered to be important) [12]. Parabolic models make up the majority of the Eulerian models [12], usually described by advection/reaction-diffusion equations, these models may incorporate either the attractive and repulsive terms or alignment terms only [2, 27, 36]. Parabolic models are more suitable for studies that involves measuring the population as a whole (e.g., mean square displacements, mean population drift) [5]. In comparison to parabolic models, hyperbolic models which are described by advection-reaction equations, may also incorporate attractive and repulsive terms or alignment terms only [9, 32]. However, these models are more suitable for studies that incorporate individual-level information (e.g., distribution of turning angles or velocity) [5]. For a more rigorous comparison between parabolic and hyperbolic models, Buono and Eftimie [5] obtained the parabolic limit of the hyperbolic model by Eftimie et al. [12] and then used group-theoretic techniques to show that any $\mathbf{O(2)}$-symmetric scalar parabolic equation with nonlocal terms can exhibit only $\mathbf{O(2)}$-symmetric steady-state bifurcations from a homogeneous equilibrium (Section 1.1).

Whereas **O(2)**-symmetric hyperbolic models which are usually described by advection-reaction equations are shown to exhibit both steady-state and Hopf bifurcations from a homogeneous equilibrium [4].

As an extension of the continuum model introduced by Pfistner [32], Eftimie et al. [12] derived a one dimensional hyperbolic model where all three interaction terms (attraction, repulsion, alignment) are incorporated in the density-dependent turning rates. This is done by considering a communication mechanism (i.e., both attraction and repulsion involve omnidirectional signals, alignment involves unidirectional signals) between neighbouring individuals. Eftimie et al. [11] further discusses the various communication mechanism models labelled **M**1–**M**5 where **M**k, $k = 1, \ldots, 5$, represent different communication mechanism models. For example, model **M**2 is a communication mechanism where all three social interaction terms depend on stimuli received from all neighbours, this model corresponds to reception of visual, auditory and olfactory signal. **M**3 represents unidirectional reception of signals that corresponds to reception of visual information. **M**4 represents omnidirectional reception of signals from individuals moving towards a reference individual, this communication mechanism corresponds to reception of directional auditory signals (Fig. 2.1). Given these communication mechanism models, numerical simulations are used to investigate the different patterns that arise when various cases are considered for different models; (a.) Only attraction and repulsion are incorporated, (b.) Only alignment is incorporated, and (c.) A full model where all three social interaction forces are incorporated in the turning rates. The numerical results are then compared to analytical predictions obtained by linearizing the equations about the homogeneous solution followed by a linear stability analysis. The results show different types of spatial patterns (i.e., stationary pulses, ripples, feathers, traveling pulse, traveling train, zigzag pulses, breathers, traveling breathers, semizigzag pulses). The symmetry properties of the hyperbolic model by Eftimie et al. [12] is investigated by Buono and Eftimie [4] where it is shown that the communication models **M**1–**M**5 defined on a finite domain $[0, L]$ with

periodic boundary conditions are *equivariant* with respect to the symmetry group $\mathbf{O(2)}$. Group-theoretic methods from [17, 18, 19] are used to investigate the linearization of the model about the $\mathbf{O(2)}$-symmetric steady-state. In particular, it was shown by Buono and Eftimie [4] that symmetry enables one to decompose the tangent space at steady-state solutions into symmetry-invariant subspaces which allows one to classify the bifurcating solutions according to their *isotropy subgroups* and determine the criticality and stability of these primary branches. These models are further extended by Eftimie [10] by considering two communication mechanisms between individuals labelled $\mathbf{M}i$ & $\mathbf{M}j$. The use of two communication mechanisms allows for the splitting of the population into two subpopulations u and v where each subpopulation is equipped with communication mechanism $\mathbf{M}i$ and $\mathbf{M}j$, respectively. Given this approach, it is observed that; "*When two subpopulations use different communication mechanisms to interact with each other, the resulting group patterns might not be at all related to the patterns exhibited by each subpopulation alone*". The use of a two-communication mechanism model can also lead to a chaotic behaviour whereas, the one-communication mechanism is associated with regular behaviour [10].

The aim of this thesis is to focus on the two-communication mechanism model on a one-dimensional spatial domain introduced by Eftimie [10] and use group-theoretic techniques to investigate the role of model symmetries on the formation of various patterns near bifurcation. To this end, we follow the approach of Buono and Eftimie [4, 5] to show that all two-communication mechanism models labelled $\mathbf{M}i$ & $\mathbf{M}j$ with periodic boundary conditions on the domain $[0, L]$ are symmetric with respect to the group actions induced by the group $\mathbf{O(2)}$. Given this symmetry perspective, we use the group-theoretic techniques described by Golubitsky and Stewart [18], Golubitsky et al. [19] and show that the phase space of the linearization about the $\mathbf{O(2)}$-symmetric homogeneous steady-state solution can be decomposed into finite dimensional invariant subspaces (Section 1.1). Also, the process of *symmetry-breaking* of the fully symmetric equilibrium solution at bifurcation (steady-state and Hopf) as described in [18, 19] is demonstrated for this system. In partic-

ular, we describe the bifurcating solutions and classify them into their respective *isotropy subgroups*, we then plot the eigenfunctions for each solution type to interpret the patterns obtained as space-time diagrams. We also include a short description of the *Liapunov-Schmidt reduction* as described in [17, 18], the reduction itself is not done in this thesis however it is well understood for a system with $\mathbf{O(2)}$-symmetry. The Liapunov-Schmidt reduction allows one to obtain a polynomial form of the equations from which the bifurcating branches are obtained which can lead to information necessary to determine the criticality and stability of the bifurcating branches.

The main feature of this thesis is the $\mathbf{O(2)}$-symmetry of the bifurcating system (Section 2.2). In particular, the presence of the symmetry impose strong restrictions on the form of the bifurcating branches and the conditions at which steady-state or Hopf bifurcation take place. In fact, the bifurcating branches (i.e., stationary pulse, rotating wave, standing wave) obtained from the symmetry-breaking of the fully-symmetric spatially homogeneous steady-state correspond to the classical patterns (i.e., stationary pulse, traveling trains) obtained via numerical simulations from the one-communication mechanism model by [11, 12]. To be able to investigate this feature and obtain more information about bifurcating solutions for an $\mathbf{O(2)}$-symmetric system, we require knowledge of group-representation theory. We note that, we focus on *geometric methods* as noted by Golubitsky et al. [19] which are designed to extract as much information as possible from *linear* data [19]. In the following section we give a brief summary of the group-theoretic preliminaries from the books [17, 18, 19] that is used throughout this thesis.

1.1 Preliminary Background Material

When discussing symmetry groups, it is important to determine how a group *acts* on a space [18, 19]. We start this discussion with an introduction to various groups. In this thesis we consider *Lie groups*.

Definition 1.1.1. *A Lie group is a smooth manifold* Γ *which is also a group and such that the group product*

$$\Gamma \times \Gamma \to \Gamma$$

and the inverse map $\Gamma \to \Gamma$ *are smooth.*

In particular we consider *matrix Lie groups* which are defined to be a closed subgroup of the group of all nonsingular $n \times n$ matrices over $\mathbb{R}$ denoted as $\mathbf{GL(n)}$ [21]. In this thesis, we follow the convention of Golubitsky et al. [19] where Lie groups are referred by the name of its associated abstract group (i.e., the two-element group $\mathbf{Z}_2 = \{\pm 1\}$ is isomorphic to the subgroup $\{I_n, -I_n\}$ where I_n is the $n \times n$ identity matrix). Below are the Lie groups that will be seen in the upcoming chapters as defined in [19];

(a) The 2-dimensional *orthogonal group*: $\mathbf{O(2)}$ consists of all 2×2 matrices satisfying

$$AA^T = I_n.$$

This group is generated by the action κ with

$$\kappa = \begin{bmatrix} 1 & 0 \\ 0 & -1 \end{bmatrix}$$

and the special orthogonal group $\mathbf{SO(2)}$.

(b) The *special orthogonal group*: $\mathbf{SO(2)}$ consists of all $A \in \mathbf{O(2)}$ such that $\det A = 1$. In particular this group consists of planar rotations

$$R_\theta = \begin{bmatrix} \cos\theta & -\sin\theta \\ \sin\theta & \cos\theta \end{bmatrix},$$

$\mathbf{SO}(2)$ may be identified with the *circle group* $\mathbf{S}^1$ using the identification $R_\theta \mapsto \theta$.

(c) The *cyclic group* of order r: $\mathbf{Z}_r$ may be identified with the group of 2×2 matrices $R_{2\pi/r}$.

(d) The *dihedral group* of order $2n$: $\mathbf{D}_n$ is generated by $R_{2\pi/n}$ together with κ.

After the description of various Lie groups, we proceed to the discussion on how these groups act on a vector space. Let Γ be a Lie group and V be a vector space then Γ acts (*linearly*) on V if there exists a continuous mapping (*representation of* Γ *on* V) $\rho : \Gamma \times V \to V$. That is,

$$(\gamma, v) \mapsto \gamma \cdot v \tag{1.1.1}$$

such that:

(a) For each $\gamma \in \Gamma$ the mapping $\rho_\gamma : V \to V$ defined by $\rho_\gamma(v) = \gamma \cdot v$ is linear, and

(b) If $\gamma_1, \gamma_2 \in \Gamma$ then $\gamma_1 \cdot (\gamma_2 \cdot v) = (\gamma_1 \gamma_2) \cdot v$.

It is stated in [19] that the study of representations of Lie groups is often made easier by observing that it decomposes into a direct sum of simpler representations called *isotypic components of* V, which are *irreducible*. Theorem 2.5 from [19] states that this decomposition always exists, however this decomposition is not unique in general but the sources of nonuniqueness can be described and controlled. As before, we consider a Lie group Γ acting on a vector space V then a subspace $W \subset V$ is Γ-*invariant* if;

$$\gamma \cdot w \in W, \qquad\qquad \forall w \in W,\ \gamma \in \Gamma.$$

A representation of Γ on V is Γ-*irreducible* or irreducible if the only Γ-invariant subspaces of V are $\{0\}$ and itself.

We now begin a discussion on the symmetries of systems of partial differential equations

(PDE)s and its solutions. Suppose we have a parameterized system of PDEs

$$\frac{\partial \mathbf{u}}{\partial t} = F(\mathbf{u}, \lambda) \tag{1.1.2}$$

where $F : \mathcal{X} \times \mathbb{R}^r \to \mathcal{Y}$, with Banach spaces $\mathcal{X}, \mathcal{Y}$ and $F \in C^\infty$. Also, suppose Γ is a Lie group acting on $\mathcal{X}$, then the system (1.1.2) is symmetric under the action of Γ if given a solution $\mathbf{u}$ then $\gamma \cdot \mathbf{u}$ is a solution of (1.1.2) for $\gamma \in \Gamma$. If so, we say that system (1.1.2) is Γ-*equivariant* or Γ-*symmetric*. Γ-equivariant systems satisfies

$$F(\gamma \cdot \mathbf{u}, \lambda) = \gamma \cdot F(\mathbf{u}, \lambda). \tag{1.1.3}$$

A symmetry of a solution of (1.1.2) is defined as $\sigma \in \Gamma$ such that σ leaves the solution $\mathbf{u}$ fixed, that is,

$$\sigma \cdot \mathbf{u} = \mathbf{u}.$$

The set of all symmetries of the solution $\mathbf{u}$ forms a subgroup of Γ called *isotropy subgroup of* $\boldsymbol{u}$, and will be denoted as

$$\Sigma_{\mathbf{u}} := \{\gamma \in \Gamma \mid \gamma \cdot \mathbf{u} = \mathbf{u}\} \subseteq \Gamma. \tag{1.1.4}$$

The subspace of $\mathcal{X}$ that are fixed by the elements of the groups Σ called *fixed-point subspace*

$$\mathrm{Fix}(\Sigma) := \{\mathbf{u} \in \mathcal{X} \mid \sigma \cdot \mathbf{u} = \mathbf{u},\ \forall \sigma \in \Sigma\}. \tag{1.1.5}$$

The *group orbit of* $\boldsymbol{u}$ is defined as

$$\Gamma_{x(t)} := \{\mathbf{v} \in \mathcal{X} \mid \mathbf{v} = \gamma \cdot \mathbf{u},\ \gamma \in \Gamma\}. \tag{1.1.6}$$

One of the goals of this thesis is to demonstrate the generic existence of bifurcating

branches of steady-state and periodic solutions corresponding to special classes of isotropy subgroups for the two-communication mechanism model for animal aggregation introduced by Eftimie [10]. To demonstrate this, we give a brief discussion on how solutions (steady-state and periodic) with specific symmetries can be obtained by restricting our search to the fixed-point subspaces of special isotropy subgroups, in particular *axial* and $\mathbb{C}$-*axial subgroups* which we now describe.

Consider a Γ-equivariant system of the form (1.1.2) with a Γ-symmetric equilibrium $(\mathbf{x}_0, \lambda_0)$ and let $L = (dF)_{\mathbf{x}_0,\lambda_0}$ be its linearization. Suppose we want to find bifurcating branches of steady-states with symmetry $\Sigma \subset \Gamma$, then as shown by Golubitsky et al. [19] $\ker(L) \neq \{0\}$ and such solutions must lie in

$$\mathrm{Fix}(\Sigma) := \{y \in \ker L \mid \sigma \cdot y = y, \forall \sigma \in \Sigma\}.$$

Restricting system (1.1.2) to the fixed-point subspace of Σ leads to a system of m equations of the form

$$g(y, \lambda) = 0$$

where $g : \mathrm{Fix}(\Sigma) \times \mathbb{R} \to \mathrm{Fix}(\Sigma)$ which then leads to our target Σ-symmetric solutions. We note that g is Σ-equivariant and a special case of this restriction is when $\mathrm{Fix}(\Sigma)$ is an *axial subgroup*, that is,

$$\dim \mathrm{Fix}(\Sigma) = 1.$$

As described by Golubitsky et al. [19], the fundamental observation about axial subgroups is the *Equivariant Branching Lemma*. Which states that generically for axial subgroups Σ, there exists a unique branch of Σ-symmetric nontrivial steady-state solutions to the system $g = 0$. The Equivariant Branching Lemma and its application to the model by Eftimie [10] is further discussed in Section 4.1. Analogous to the steady-state case, the generic existence of branches of periodic solutions can be shown by restricting the Γ-symmetric

vector field (1.1.2) to the fixed-point subspace of Σ. However, this restriction was shown by Golubitsky et al. [19] to be a weak result (e.g., symmetry Γ may force multiple purely imaginary eigenvalues). To address this issue, we consider the autonomous nature of the model which introduces a temporal symmetry to the system. In particular, we now restrict the Γ-symmetric vector field to the eigenspace that corresponds to the purely imaginary eigenvalues which exhibits $\Gamma \times \mathbf{S}^1$-symmetry. We then seek bifurcating branches of periodic solutions with symmetry group $\Sigma \subset \Gamma \times \mathbf{S}^1$ by restricting the vector field in $\mathrm{Fix}(\Sigma)$. As a counterpart to axial subgroups, we define the $\mathbb{C}$-*axial* subgroup Σ that satisfies the following

$$\dim \mathrm{Fix}(\Sigma) = 2.$$

As an analog to the Equivariant Branching Lemma, the *Equivariant Hopf Theorem* [18, 19] guarantees the existence of branches of periodic solutions corresponding to $\mathbb{C}$-axial isotropy subgroups of $\Gamma \times \mathbf{S}^1$. The Equivariant Hopf Theorem and its application to the model is further discussed in Section 4.2.

This thesis is organized as follows; In Chapter 2 the model is presented along with its underlying parts. We describe the communication mechanism models that are introduced by Eftimie et al. [11]. In this thesis, we consider the two-communication mechanism model **M**3 & **M**4. The $\mathbf{O(2)}$-symmetry of the model is shown and the actions induced by the group $\mathbf{O(2)}$ are defined. This chapter also contains a discussion of the $\mathbf{O(2)}$-symmetric homogeneous steady-state solution of the model. In Chapter 3, we discuss the linearization of the model about the fully symmetric steady-state solutions shown in Chapter 2. We describe the *isotypic decomposition* of the phase space X of the linear operator $\mathcal{L}$. We then show the computation to obtain an expression $\mathcal{L}_n$ which is a restriction of $\mathcal{L}$ along the *isotypic components* of $\mathbf{O(2)}$ action. We end Chapter 3 with the discussion of the critical eigenvalues of $\mathcal{L}_n$ where we show conditions at which $\mathcal{L}_n$ may admit zero and purely imaginary eigenvalues. We also display the neutral stability curves in the parameter space

(q_a, q_r) which gives us the parameter values such that symmetry-breaking occurs. Chapter 4 starts with the discussion of symmetry breaking due to steady-state bifurcations, here we introduce the Equivariant Branching Lemma and demonstrate how a *fully-symmetric* steady-state solution can break symmetry. We then discuss symmetry-breaking in Hopf bifurcation and introduce the counter-part of the Equivariant Branching Lemma at a Hopf bifurcation called Equivariant Hopf Theorem. In this chapter a brief generic description of the Liapunov-Schmidt reduction is given. We also give a description and display the plots of the eigenfunctions for each solution type. A discussion on the general form of the equivariant mappings from the branches of solutions found from the symmetry-breaking at steady-state and Hopf bifurcations is done in Chapter 4.

Chapter 2

Model Description

In this thesis we use the same nonlocal model for self-ogranized aggregations that was derived by Eftimie [10] which incorporates not only social interactions but also different communication mechanisms among the individuals within the population. Throughout this thesis the general approach of Buono and Eftimie [4], Eftimie [10] are followed, the assumptions that were taken in the mentioned articles are extended to this model. First, the individuals in a population are assumed to communicate via two different mechanisms depending on their own physiological characteristics (i.e., directions at which individuals sends/receives the information coming from neighbouring individuals [10]). Figure 2.1 shows the different communication mechanisms that are considered, in this thesis we only study the model **M**3 & **M**4 as described by Eftimie [10]. Where model **M**3 assigns reference individuals at position x to receive information through *visual signals* from the neighbours at position $x+s$ only, this includes individuals moving towards and away from our reference individuals. Whereas, model **M**4 assigns reference individuals at position x to receive *auditory signals* from individuals at positions $x \pm s$ that are travelling towards position x.

The use of two different communication mechanisms by an animal population enables us to split the population into two subpopulations u and v, where each subpopulation is assigned its own communication mechanism. In particular, we assign subpopulations u and

v the communication mechanisms **M**3 and **M**4, respectively. As in [12] the spatial domain is assumed to be much longer that wide and we focus only on one spatial dimension from $[0, L]$.

This chapter is organized as follows; the model for the evolution of the densities of left and right-moving individuals, its underlying parts, initial and boundary conditions are described in Section 2.1. The existence of the **O(2)**-symmetry of the model is discussed in Section 2.2. Lastly, the spatially homogeneous steady-state solutions and their symmetry properties are discussed in Section 2.3.

2.1 The Model

The evolution of densities of the left and right-moving individuals (*e.g.*, $f^{\pm}(x,t)$) for $f \in \{u, v\}$ in one spatial dimension is described by a system of PDEs for functions of the form

$$\mathbf{u}(x,t) = \left(u^+(x,t), u^-(x,t), v^+(x,t), v^-(x,t)\right),$$

with

$$\frac{\partial u^+}{\partial t} + \gamma \frac{\partial u^+}{\partial x} = -\lambda_u^+[u^+, u^-, v^+, v^-]u^+(x,t) + \lambda_u^-[u^+, u^-, v^+, v^-]u^-(x,t), \tag{2.1.1a}$$

$$\frac{\partial u^-}{\partial t} - \gamma \frac{\partial u^-}{\partial x} = \lambda_u^+[u^+, u^-, v^+, v^-]u^+(x,t) - \lambda_u^-[u^+, u^-, v^+, v^-]u^-(x,t), \tag{2.1.1b}$$

$$\frac{\partial v^+}{\partial t} + \gamma \frac{\partial v^+}{\partial x} = -\lambda_v^+[u^+, u^-, v^+, v^-]v^+(x,t) + \lambda_v^-[u^+, u^-, v^+, v^-]v^-(x,t), \tag{2.1.1c}$$

$$\frac{\partial v^-}{\partial t} - \gamma \frac{\partial v^-}{\partial x} = \lambda_v^+[u^+, u^-, v^+, v^-]v^+(x,t) - \lambda_v^-[u^+, u^-, v^+, v^-]v^-(x,t), \tag{2.1.1d}$$

with initial condition $\mathbf{u}(x,0) = \left(u_0^+(x), u_0^-(x), v_0^+(x), v_0^-(x)\right)$ and a constant speed γ at which the individuals in each subpopulation travel.

The density-dependent turning functions $\lambda_{u,v}^{\pm}[u^{\pm}, v^{\pm}]$ describe the social response of an

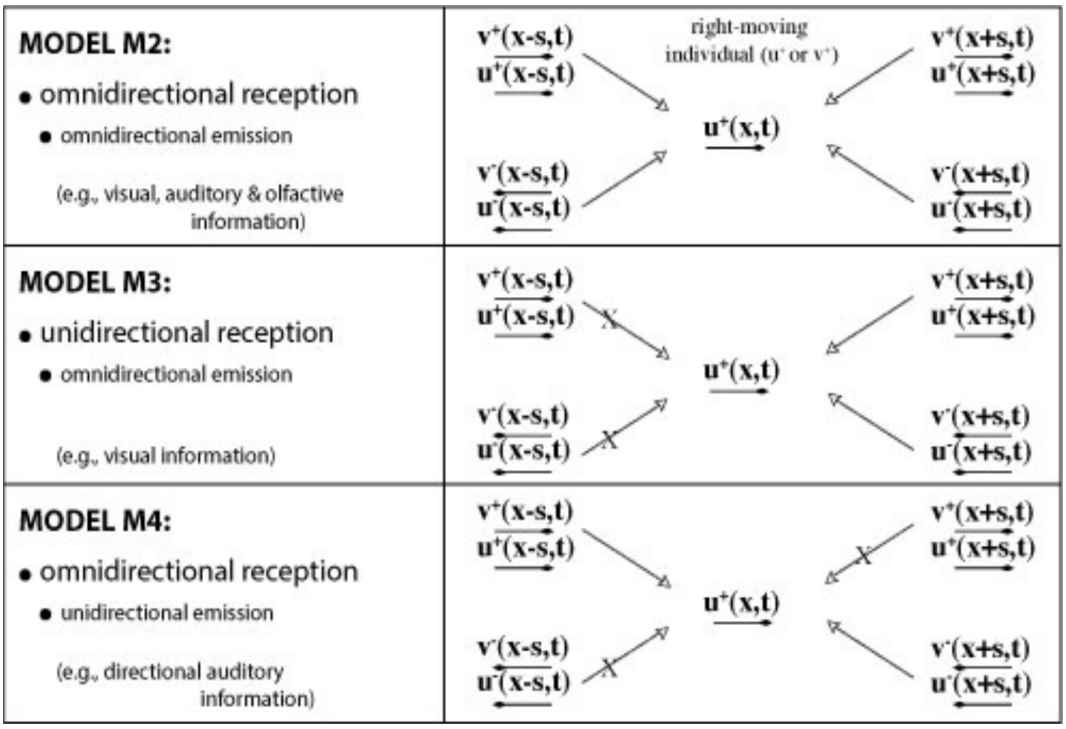

Figure 2.1: A graphical description of the three different communication mechanisms introduced by Eftimie et al. [11] that is being experienced by right moving individuals u^+ (v^+) positioned at (x,t). Following the notation from [11], the solid horizontal arrows indicate the direction at which the reference individuals move, while the slanted arrows describe the information received from neighbors and the "X" on the arrows means that no information is received from that particular direction.

individual to the signals received from its neighbors [4], it is defined as

$$\begin{aligned}\lambda^{\pm}_{u,v}[u^{\pm},v^{\pm}] &= \lambda_1 + \lambda_2 f\left(y_r^{u,v,\pm}\left[u^{\pm},v^{\pm}\right] - y_a^{u,v,\pm}\left[u^{\pm},v^{\pm}\right] + y_{al}^{u,v,\pm}\left[u^{\pm},v^{\pm}\right]\right)\\ &= \underbrace{\left[\lambda_1 + \lambda_2 f(0)\right]}_{\text{Baseline Random Turning Rate}} + \underbrace{\lambda_2\left[f\left(y_r^{u,v,\pm} - y_a^{u,v,\pm} + y_{al}^{u,v,\pm}\right) - f(0)\right]}_{\text{Bias Turning Rate}}. \quad (2.1.2)\end{aligned}$$

The subscripts u, v distinguish the turning function for the individuals belonging to subpopulations u and v, while the superscripts $(\pm)$ determine the turning rate of the individuals moving right to left $(+)$ and left to right $(-)$. In this thesis we use the same function f as in [12], where f is a positive, increasing, bounded function and it is is defined

as

$$f(y) = \frac{1}{2}\left(1 + \tanh(y - y_0)\right). \tag{2.1.3}$$

The parameter y_0 is chosen so that $f(0) \approx 0$, which implies that when there are no neighbours (i.e., $y = 0$) the turning rate is given by λ_1. Similar to the approach of [4, 10, 12, 13], we set $y_0 = 2$ and the terms $\lambda_1 + \lambda_2 f(0)$ and $\lambda_2\left(f(\mathbf{y}) - f(0)\right)$ from Eq. (2.1.2), where $\mathbf{y} = y_r^{u,v,\pm,} - y_a^{u,v,\pm} + y_{al}^{u,v,\pm}$, describe the *baseline random turning* and *bias random turning rates*, respectively [12]. For small $f(0)$, the baseline random turning rate is approximated by λ_1 and the bias random turning rate is approximated by $\lambda_2 f(\mathbf{y})$. In the following, the values of λ_1 and λ_2 are fixed.

The social interaction terms $y_j^{u,v,\pm} j \in \{r, a, al\}$ model the nonlocal interactions among the individuals in a population. The subscripts $\{r, a, al\}$ represent the following social responses between individuals; (r) *repulsion* from nearby neighbours, (a) *attraction* towards individuals that are far away and (al) *alignment* with neighbours at intermediate distances [4]. Table 2.1 provides a description of these interaction terms for the communication mechanism models **M**2–**M**4. Notice how the interaction terms depend on the spatial distance between individuals and the communication mechanisms used by each subpopulation. For example, consider the social interaction terms for right-moving individuals equipped with communication mechanism model **M**3. The attraction or repulsion terms are defined as

$$y_{r,a}^{u,+} = q_{r,a} \int_0^\infty K_{r,a}(s)\left(u(x+s) + v(x+s)\right) \mathrm{d}s,$$

with $f(x+s) = f^+(x+s) + f^-(x+s),\ f \in \{u, v\}$. These interaction terms describe how the information gathered from the left/right-moving individuals at position $x + s$ contribute to the attraction/repulsion of the reference individual to/from one group from either direction. Whereas the alignment term for the right-moving individuals defined as

$$y_{al}^{u,\pm} = q_{al} \int_0^\infty K_{al}(s)\left(u^-(x+s) + v^-(x+s) - u^+(x+s) - v^+(x+s)\right) \mathrm{d}s$$

Communication models	**Interaction terms for models Mj, $j = 2, 3, 4$** Attraction ($y_a^{\mathbf{M}j,\pm}$), Repulsion ($y_r^{\mathbf{M}j,\pm}$), Alignment ($y_{al}^{Mj,\pm}$)
M2	$y_{r,a}^{\mathbf{M2},\pm} = q_{r,a}\int_0^\infty K_{r,a}(s)\,(u(x\pm s)+v(x\pm s)-u(x\mp s)-v(x\mp s))\,\mathrm{d}s$ $y_{al}^{M2,\pm} = q_{al}\int_0^\infty K_{al}(s)(u^{\mp}(x\mp s)+u^{\mp}(x\pm s)+v^{\mp}(x\mp s)+v^{\mp}(x\pm s)$ $-u^{\pm}(x\mp s)-u^{\pm}(x\pm s)-v^{\pm}(x\mp s)-v^{\pm}(x\pm s))\,\mathrm{d}s$
M3	$y_{r,a}^{\mathbf{M3},\pm} = q_{r,a}\int_0^\infty K_{r,a}(s)\,(u(x\pm s)+v(x\pm s))\,\mathrm{d}s$ $y_{al}^{M3,\pm} = q_{al}\int_0^\infty K_{al}(s)\,\big(u^{\mp}(x\pm s)+v^{\mp}(x\pm s)-u^{\pm}(x\pm s)-v^{\pm}(x\pm s)\big)\,\mathrm{d}s$
M4	$y_{r,a}^{\mathbf{M4},\pm} = q_{r,a}\int_0^\infty K_{r,a}(s)\,\big(u^{\mp}(x\pm s)+v^{\mp}(x\pm s)-u^{\pm}(x\mp s)-v^{\pm}(x\mp s)\big)\,\mathrm{d}s$ $y_{al}^{M4,\pm} = q_{al}\int_0^\infty K_{r,a}(s)\,\big(u^{\mp}(x\pm s)+v^{\mp}(x\pm s)-u^{\pm}(x\mp s)-v^{\pm}(x\mp s)\big)\,\mathrm{d}s$
M2&M3	$y_{r,a,al}^{u,\pm} = y_{r,a,al}^{\mathbf{M2},\pm}, \quad y_{r,a,al}^{v,\pm} = y_{r,a,al}^{\mathbf{M3},\pm}$
M2&M4	$y_{r,a,al}^{u,\pm} = y_{r,a,al}^{\mathbf{M2},\pm}, \quad y_{r,a,al}^{v,\pm} = y_{r,a,al}^{\mathbf{M4},\pm}$
M3&M4	$y_{r,a,al}^{u,\pm} = y_{r,a,al}^{\mathbf{M3},\pm}, \quad y_{r,a,al}^{v,\pm} = y_{r,a,al}^{\mathbf{M4},\pm}$

Table 2.1: Nonlocal social interaction terms $\big(y_j^{\pm}, j \in \{r,a,al\}\big)$. The constants $q_{r,a,al}$ describe the magnitudes of the repulsive,attractive and alignment interactions, respectively. The kernels $K_{r,a,al}$ describe the spatial ranges for each of the social interactions. We use the same normalised kernels $K_j(s) = \frac{1}{2\pi m_j^2} e^{-(s-s_j)^2/(2m_j^2)}, j \in \{r,a,al\}$ as in [11], where s_j represents half of the length of the interaction ranges and $m_j = s_j/8$ represents the width of the interaction kernels. The domain is set to be $L = 10$ and the range of the interactions have lengths $s_a = 1, s_{al} = \frac{1}{2}, s_r = \frac{1}{4}$.

shows how the reference individuals estimate the difference between the density of individuals moving in the same direction compared to the ones moving in the opposite direction before triggering a response to change or keep its initial orientation. The parameters $q_j, j \in \{r,a,al\}$ that appear in front of the integrals describe the magnitude of the interactions. The spatial distance distance between individuals is modelled by the spatial kernels $K_j(s), j \in \{r,a,al\}$, these indicate whether the interactions take place inside the *repulsion range* (K_r), *attraction range* (K_a) and *alignment range* (K_{al}). Similar to [4] we consider

the translated Gaussian kernels

$$K_j(s) = \frac{1}{2\pi m_j^2} e^{-(s-s_j)^2/(2m_j^2)}, \tag{2.1.4}$$

where s_j represent the length of the interaction ranges and $m_j = s_j/8$ represent the width of the interaction kernels for $j \in \{r, a, al\}$. Since we are considering a large finite domain of $[0, L]$, we follow the approach of [12] where the kernels are chosen such that more than 98% of the kernels is small with respect to the length of the domain. This allows us to approximate the interactions on an infinite domain using a finite domain with periodic boundary conditions. In fact, it is shown in [12] that this approximation is valid. We note that the small overlap between the kernels (e.g., $\sim 2\%$) enables us to model quite distinct interaction ranges which allows for a better comparison with individual-based models [13], given this small overlap we can distinguish the social interaction effects of one neighbour from another and determine how these affect the turning function of a reference individual. Also, the effects of these interactions are assumed to be additive, i.e., the repulsion and attraction interaction terms come in with opposite signs. The integrals in Table 2.1 describe the effect of each social interaction term on the turning rates for each of the communication mechanisms described in Fig. 2.1. Note that, we assume that the individuals behave in a similar way upon receiving information from their neighbours from their own subpopulation (u) and the other subpopulation (v), to ensure that there is no discriminatory behaviour toward individuals belonging to the other subpopulation [10]. Lastly, periodic boundary conditions on a finite domain of length L are imposed so that

$$u^{\pm}(0,t) = u^{\pm}(L,t), \qquad v^{\pm}(0,t) = v^{\pm}(L,t). \tag{2.1.5}$$

2.2 O(2)-Symmetry of the Model

The periodic boundary conditions (2.1.5) have strong implications on the model's symmetry. In particular, conditions (2.1.5) implies the **O(2)**-symmetry of the communication mechanism models from Table 2.1. To show this, we start by introducing the following group actions that act on functions of the form

$$\mathbf{u}\left(x,t\right)=\left(u^{+}\left(x,t\right),u^{-}\left(x,t\right),v^{+}\left(x,t\right),v^{-}\left(x,t\right)\right) \tag{2.2.1}$$

satisfying (2.1.5). First, the *translation operator* $T_z : \mathbb{R} \to \mathbb{R}$, which translates functions by $z \in \mathbb{R}$, the action of this operator is defined as

$$T_z(x) = x - z,$$

and the group of all translations T_z is isomorphic to $\mathbb{R}$. However, due to the condition (2.1.5), the action of the translation group on the spatial domain of the functions of the form (2.2.1) is isomorphic to $\mathbb{R}/L\mathbb{Z} \simeq \mathbf{SO(2)}$. This enables us to use $\theta \in [0, L]$ to parameterize **SO(2)** and use it as the translator operator as follows

Definition 2.2.1. *The translation operator $\theta \in [0, L]$ acts on L-periodic functions of the form (2.2.1) via its spatial domain*

$$\theta \cdot \boldsymbol{u}(x,t) = \boldsymbol{u}(x-\theta,t). \tag{2.2.2}$$

Next, we introduce a $\mathbb{Z}_2$ action on the functions of the form (2.2.1)

Definition 2.2.2. *The reflection operator κ sends the right-moving individuals at position*

x to the left-moving individuals at position $L-x$ and vice versa,

$$\kappa\cdot(u^+(x,t),u^-(x,t),v^+(x,t),v^-(x,t)) = \\ \big(u^-(L-x,t),u^+(L-x,t),v^-(L-x,t),v^+(L-x,t)\big)\,. \tag{2.2.3}$$

To show the model's **O(2)**-symmetry we first rewrite (2.1.1) as

$$\frac{\partial u^+}{\partial t} = -\lambda_u^+[u^+,u^-,v^+,v^-]u^+ + \lambda_u^-[u^+,u^-,v^+,v^-]u^- - \gamma\frac{\partial u^+}{\partial x} = F_1(\mathbf{u},\mu)\,, \tag{2.2.4a}$$
$$\frac{\partial u^-}{\partial t} = \lambda_u^+[u^+,u^-,v^+,v^-]u^+ - \lambda_u^-[u^+,u^-,v^+,v^-]u^- + \gamma\frac{\partial u^-}{\partial x} = F_2(\mathbf{u},\mu)\,, \tag{2.2.4b}$$
$$\frac{\partial v^+}{\partial t} = -\lambda_v^+[u^+,u^-,v^+,v^-]v^+ + \lambda_v^-[u^+,u^-,v^+,v^-]v^- - \gamma\frac{\partial v^+}{\partial x} = F_3(\mathbf{u},\mu)\,, \tag{2.2.4c}$$
$$\frac{\partial v^-}{\partial t} = \lambda_v^+[u^+,u^-,v^+,v^-]v^+ - \lambda_v^-[u^+,u^-,v^+,v^-]v^- + \gamma\frac{\partial v^-}{\partial x} = F_4(\mathbf{u},\mu)\,. \tag{2.2.4d}$$

We note that the social interaction terms for a right moving individuals (+) from population u or v are transformed as follows under the action of κ

$$\kappa\cdot y_j^{u,v,+} = q_j\int_0^\infty K_j(s)\Big(u(L-(x+s))+v(L-(x+s))\Big)\,\mathrm{d}s = y_j^{u,v,-}(L-x),\ j=r,a,$$
$$\kappa\cdot y_{al}^{u,v,+} = q_{al}\int_0^\infty K_{al}(s)\Big(u^-(L-x-s)+v^+(L-x-s)- \\ u^-(L-x-s)-v^-(L-x-s)\Big)\,\mathrm{d}s = y_{qa}^{u,v,-}(L-x).$$

As a consequence, the turning rate attached to $u^+(v^+)$ at x becomes the turning rate of $u^-(v^-)$ at $L-x$, that is,

$$\kappa\cdot\lambda_{u,v}^+(x) = \lambda_{u,v}^-(L-x).$$

Due to the θ-invariance of the differential operator ∂_x and the turning functions $\lambda_{u,v}^\pm$

$$\theta\cdot\lambda_{u,v}^\pm\left[u^+(x,t),u^-(x,t),v^+(x,t),v^-(x,t)\right] := \lambda_1+\lambda_2 f\Big(y_r^{u,v,\pm}\left[u^\pm(x-\theta),v^\pm(x-\theta)\right] \\ -y_a^{u,v,\pm}\left[u^\pm(x-\theta),v^\pm(x-\theta)\right]+y_{al}^{u,v,\pm}\left[u^\pm(x-\theta),v^\pm(x-\theta)\right]\Big).$$

Making the following change of variables $\tilde{x} = x - \theta$ proves the θ-invariance of $\lambda^{\pm}_{u,v}[u^{\pm}, v^{\pm}]$. Then it follows that system (2.2.4) is θ-equivariant, that is,

$$F_i\left[\theta \cdot \mathbf{u}\left(x,t\right)\right] = \theta \cdot F_i\left[\mathbf{u}\left(x,t\right)\right], \qquad\qquad i = 1,2,3,4.$$

Since $\theta \circ \kappa = \kappa \circ (-\theta)$, then we obtain the group $\mathbf{O(2)} \simeq \mathbf{SO(2)} \rtimes \mathbb{Z}_2(\kappa)$ acting on the spatial domain of $\mathbf{u}\left(x,t\right)$. We note that $\mathbf{SO(2)} \rtimes \mathbb{Z}_2(\kappa)$ denotes a semi-direct product between the groups $\mathbf{SO(2)}$ and $\mathbb{Z}_2(\kappa)$. That is, every $\gamma \in \mathbf{O(2)}$ can be written uniquely as $\gamma = \theta\kappa$ for $\theta \in \mathbf{SO(2)}$, $\kappa \in \mathbb{Z}_2(\kappa)$, we also note that $\mathbf{SO(2)}$ is a normal subgroup of $\mathbf{O(2)}$ and $\mathbf{SO(2)} \cap \mathbb{Z}_2(\kappa) = \{e\}$. The $\mathbf{O(2)}$-equivariance of the model follows since for a given solution $\mathbf{u}\left(x,t\right)$ of (2.1.1) then $\theta \cdot \mathbf{u}(x,t)$ and $\kappa \cdot \mathbf{u}(x,t)$ are solutions as well. We summarize the results in the following statement:

Proposition 2.2.3. *The system of partial differential equations (2.1.1) labelled* ***M2–M4****, defined on* $[0, L]$ *with periodic boundary conditions*

$$u^{\pm}(0,t) = u^{\pm}(L,t), \qquad\qquad v^{\pm}(0,t) = v^{\pm}(L,t)$$

are ***O(2)****-equivariant. Where* ***O(2)*** *acts on solutions of (2.1.1) via the actions (2.2.2) and (2.2.3).*

2.3 Spatially Homogeneous Steady-States

We start this section by discussing the spatially homogeneous steady-states of the one-population models described in [4, 12], we then extend those ideas to our two-communication mechanism model. It is shown in [12] that the models that incorporate only one communication mechanism (i.e., $v = 0$) can display up to five spatially homogeneous steady-states of the form $(u^+, u^-) = (u^\star, A - u^\star)$, where $A = \frac{1}{L}\int_0^\infty \left(u^+\left(x,t\right) + u^-\left(x,t\right)\right) \mathrm{d}x$ represents

the total population density of the one-population models. It is also discussed in [12] that the steady-states $(u^+, u^-) = (A/2, A/2)$ exists for all parameter values, and the remaining four possible steady states are of the form $(u^+, u^-) = (u^\star, A - u^\star)$. More specifically, it was shown in [12] that the spatially homogeneous steady-states generically denoted by $(u^\star, A - u^\star)$ can be any of the following pairs; $({u^\star}_1, {u^\star}_5)$, $({u^\star}_5, {u^\star}_1)$, $({u^\star}_2, {u^\star}_4)$, $({u^\star}_4, {u^\star}_2)$, $({u^\star}_3, {u^\star}_3)$. The number of steady-states can vary from one, three or five depending of the variation of the parameter values. For example, when $q_{al} = 0$ the only steady-state is $(u^+, u^-) = (A/2, A/2)$, but when $q_{al} \neq 0$ then we see the possibilities of having one, three or five steady-states [12].

The discussion of the steady-state solutions from [4] is mainly focused on the classification of the solutions based on its symmetry group. Since our model is $\mathbf{O(2)}$-symmetric, it is natural for us to follow their approach. The $\mathbf{O(2)}$-symmetry of the model implies that its solutions may exhibit some type of symmetry as well, using definitions from Chapter 1.1 we are able to classify these solutions with respect to their symmetry groups. In [4], it is shown that all steady-state solutions of the one-population model must satisfy

$$u^-(x) = u^+(x) + C$$

for some arbitrary constant C. If the system has a solution $(u^+(x), u^-(x))$ with isotropy subgroup Σ such that $(\theta, \kappa) \in \Sigma$, then by Theorem 2.2 of citepaper5 it follows that $C = 0$. Therefore, the one-population model that possesses $\mathbf{O(2)}$-symmetry admits a steady-state solution with isotropy subgroup Σ such that $(\theta, \kappa) \in \Sigma$ and it is of the form $(u^+, u^-) = (u^\star, u^\star) = (A/2, A/2)$. As mentioned above, this type of steady-state exists for all parameter values, and is fixed by $\mathbf{O(2)}$. In fact, all elements of $\mathrm{Fix}\,(\mathbf{O(2)})$ are of the form $(A/2, A/2)$ [4]. It is also important to note that the steady-states of the form $(u^\star, A - u^\star)$ are fixed by any translation (2.2.2) and therefore these type of steady-states have isotropy subgroup $\mathbf{SO(2)}$. Moreover, $\kappa \cdot (u^\star, A - u^\star) = (A - u^\star, u^\star)$, so these equilib-

ria are on the same *group orbit* [4]. Also note, in the one-population model, there exists a family of *non-homogeneous* steady-states that possess $\mathbf{D}_n$-symmetry. These solutions can be obtained from a *symmetry-breaking steady-state bifurcation* from an $\mathbf{O(2)}$-symmetric steady-state solution.

We now discuss the steady-states of the two-population model. The spatially homogeneous steady-states exhibited by system (2.1.1) are obtained by setting both the space and time derivatives of both subpopulations to zero. (i.e., $u_t^{\pm} = v_t^{\pm} = u_x^{\pm} = v_x^{\pm} = 0$). In other words, the solutions $[u_\star^+, u_\star^-, v_\star^+, v_\star^-]$ are intersection points between the curves [10]

$$\begin{aligned} 0 &= -\lambda_u^+[u_\star^+, u_\star^-, v_\star^+, v_\star^-]u_\star^+ + \lambda_u^-[u_\star^+, u_\star^-, v_\star^+, v_\star^-]u_\star^-, \\ 0 &= -\lambda_v^+[u_\star^+, u_\star^-, v_\star^+, v_\star^-]v_\star^+ + \lambda_v^-[u_\star^+, u_\star^-, v_\star^+, v_\star^-]v_\star^-. \end{aligned}$$

We define the total population densities for subpopulation u and v as

$$\begin{aligned} A_u &= \frac{1}{L}\int_0^\infty \big(u^+(x,t) + u^-(x,t)\big)\,\mathrm{d}x, \\ A_v &= \frac{1}{L}\int_0^\infty \big(v^+(x,t) + v^-(x,t)\big)\,\mathrm{d}x. \end{aligned}$$

We note that, the total population defined by $A_f,\ f \in \{u, v\}$ are conserved quantities. To show this, consider

$$\begin{aligned} \frac{\mathrm{d}}{\mathrm{d}t}A_f &= \frac{1}{L}\int_0^\infty \frac{\mathrm{d}}{\mathrm{d}t}\big(f^+(x,t) + f^-(x,t)\big)\,\mathrm{d}x \\ &= -\frac{\gamma}{L}\int_0^\infty \frac{\partial}{\partial x}\big(f^+(x,t) + f^-(x,t)\big)\,\mathrm{d}x \\ &= -\frac{\gamma}{L}\underbrace{\big[\big(f^+(L,t) - f^-(L,t)\big) - \big(f^+(0,t) - f^-(0,t)\big)\big]}_{L\text{-periodic density functions } f^{\pm}(x,t)} = 0. \end{aligned}$$

Similar to [10], we focus on the spatially homogeneous steady-state solution that exists for

all parameter values for all models

$$\left(u^+, u^-, v^+, v^-\right) = (A_u/2, A_u/2, A_v/2, A_v/2) \tag{2.3.2}$$

for some $A_u, A_v > 0$. Similar to the one-population models, the spatially homogeneous steady-states (2.3.2) have isotropy subgroup $\mathbf{O(2)}$, that is,

$$\gamma \cdot (A_u/2, A_u/2, A_v/2, A_v/2) = (A_u/2, A_u/2, A_v/2, A_v/2)\,,\ \forall \gamma \in \mathbf{O(2)}.$$

Given this fully symmetric spatially homogeneous steady-state solution, we now aim to answer the question; *Generically, for which isotropy subgroups Σ should we expect to find bifurcating branches of steady-states and periodic solutions, having Σ and $\Sigma \times \mathbf{S^1}$, respectively, as their group of symmetries?* In other words, we would like to determine what type of solutions can occur once the $\mathbf{O(2)}$-symmetric steady-state solution undergoes a symmetry-breaking bifurcation. To answer this question, we begin by linearizing the system about the steady-state (2.3.2) and apply the *Equivariant Branching Lemma* and the *Equivariant Hopf Theorem* [18, 19].

Chapter 3

Linearization of the model

It is shown in [4, 10, 11, 12] that linearizing the equations about the spatially homogeneous steady-states is the first step in studying pattern formation for the one-population model. It also leads to a better understanding of the important mechanism for pattern formation, *symmetry-breaking* [18], that occurs once a bifurcation point is crossed. In particular, having a symmetry perspective for the two-population model, we start by linearizing Eq. (2.1.1) to discuss the type of symmetries that may arise once an $\mathbf{O(2)}$-symmetric homogeneous steady-state solution breaks symmetry as it undergoes steady-state or Hopf bifurcations. We use techniques described from [17, 19] to show the conditions for the existence of new types of solutions at bifurcation.

This Chapter is organized as follows; The linearization of the Model (2.1.1) is shown in Section 3.1, this leads to the linear operator $\mathcal{L}$ which is infinite dimensional. Taking advantage of the $\mathbf{O(2)}$-symmetry of the system, we perform an isotypic decomposition of the phase space of $\mathcal{L}$ in Section 3.2 as discussed in [18, 19]. The isotypic decomposition allows us to work with the operator $\mathcal{L}_n$ that is finite-dimensional. In Section 3.3, the computation of the critical eigenvalues of $\mathcal{L}_n$ and its corresponding eigenspaces is shown and the neutral stability curves for various wave numbers are discussed.

3.1 Computation of $\mathcal{L}$

To linearize Eqs. (2.1.1), we consider small perturbations of the spatially homogeneous steady-states (2.3.2) described in Chapter 2.3;

$$\left(u^+, u^-, v^+, v^-\right) = \left(u^\star + u_1^+, u^\star + u_1^-, v^\star + v_1^+, v^\star + v_1^-\right)$$

with $u^\star = A_u/2, v^\star = A_v/2$ and $u_1^\pm, v_1^\pm \ll 1$. We then perform a Taylor series expansion of

$$\lambda_{u,v}^\pm \left[u^\star + u_1^+, u^\star + u_1^-, v^\star + v_1^+, v^\star + v_1^-\right],$$

neglecting the nonlinear terms leads to the following;

$$\begin{aligned}\lambda_u^\pm[u^\star + u_1^+, u^\star + u_1^-, v^\star + v_1^+, v^\star + v_1^-] \approx \lambda_1 + \lambda_2 f(0) + \\ \lambda_2 f'(0) \int_0^\infty \left(q_r K_r(s) - q_a K_a(s)\right) \left[u_1(x \pm s) + v_1(x \pm s) + 2\left(u^* + v^*\right)\right] \mathrm{d}s + \\ \lambda_2 f'(0) \int_0^\infty q_{al} K_{al}(s) \left[u_1^\mp(x \pm s) + v_1^\mp(x \pm s) - u_1^\pm(x \pm s) - v_1^\pm(x \pm s)\right] \mathrm{d}s,\end{aligned}$$

and

$$\begin{aligned}\lambda_v^\pm[u^\star + u_1^+, u^\star + u_1^-, v^\star + v_1^+, v^\star + v_1^-] \approx \lambda_1 + \lambda_2 f(0) + \\ \lambda_2 f'(0) \int_0^\infty \Big(q_r K_r(s) - q_a K_a(s) + q_{al} K_{al}(s)\Big) \\ \times \left[u_1^\mp(x \pm s) + v_1^\mp(x \pm s) - u_1^\pm(x \mp s) - v_1^\pm(x \mp s)\right] \mathrm{d}s.\end{aligned}$$

Substituting the perturbed homogeneous steady-states and the first-order Taylor series expansion of $\lambda_{u,v}^\pm$ into system (2.1.1) and collecting similar terms together and introduce the following notation to simplify our calculations

$$L_1 = \lambda_1 + \lambda_2 f(0), \qquad R_1 = \lambda_2 f'(0), \qquad R_2 = 2R_1, \qquad R_3 = \widetilde{A} R_1, \qquad \widetilde{A} = 2\left(u^* + v^*\right)$$

$$K_1(s) = q_r K_r(s) - q_a K_a(s) + q_{al} K_{al}(s), \qquad K_2(s) = q_r K_r(s) - q_a K_a(s) - q_{al} K_{al}(s),$$
$$K_3(s) = q_r K_r(s) - q_a K_a(s), \qquad \overline{K}_3 = \int_0^\infty K_3(s)\,\mathrm{d}s.$$

We also introduce the following operators

$$K_i^{\pm} * v(x) = \int_0^\infty K_i(s) v(x \pm s)\,\mathrm{d}s,\ i = \{1,2,3\}\,.$$

Applying these simplifications to our equations gives us the following linearized **M**3 & **M**4 model

$$\frac{\partial u_1^+}{\partial t} + \gamma \frac{\partial u_1^+}{\partial x} = -L_1(u_1^+ - u_1^-) - \overline{K}_3 R_3(u_1^+ - u_1^-) - R_1 u^*[K_2^+ * u_1^+ - K_2^- * u_1^-$$
$$+ K_2^+ * v_1^+ - K_2^- * v_1^- - K_1^- * u_1^+ + K_1^+ * u_1^- - K_1^- * v_1^+ + K_1^+ * v_1^-] \tag{3.1.1a}$$
$$\frac{\partial u_1^-}{\partial t} - \gamma \frac{\partial u_1^-}{\partial x} = L_1(u_1^+ - u_1^-) + \overline{K}_3 R_3(u_1^+ - u_1^-) + R_1 u^*[K_2^+ * u_1^+ - K_2^- * u_1^-$$
$$+ K_2^+ * v_1^+ - K_2^- * v_1^- - K_1^- * u_1^+ + K_1^+ * u_1^- - K_1^- * v_1^+ + K_1^+ * v_1^-] \tag{3.1.1b}$$
$$\frac{\partial v_1^+}{\partial t} + \gamma \frac{\partial v_1^+}{\partial x} = -L_1(v_1^+ - v_1^-) + R_2 v^* \left[K_1^- * u_1^+ - K_1^+ * u_1^- + K_1^- * v_1^+ - K_1^+ * v_1^-\right] \tag{3.1.1c}$$
$$\frac{\partial v_1^-}{\partial t} - \gamma \frac{\partial v_1^-}{\partial x} = L_1(v_1^+ - v_1^-) - R_2 v^* \left[K_1^- * u_1^+ - K_1^+ * u_1^- + K_1^- * v_1^+ - K_1^+ * v_1^-\right] \tag{3.1.1d}$$

The linear operator $\mathcal{L}$ associated with system (3.1.1) can be written as

$$\mathcal{L} = \mathcal{L}_0 - \gamma \mathcal{L}_d,$$

where $\mathcal{L}_d = \operatorname{diag}(\partial_x, -\partial_x, \partial_x, -\partial_x)$ and $\mathcal{L}_0$ is given by the following 4×4 matrix

$$\mathcal{L}_0 = \begin{bmatrix} [\mathcal{L}_0]_{1,1} & [\mathcal{L}_0]_{1,2} & -R_1 u^\star \left[K_2^+ * \cdot - K_1^- * \cdot\right] & R_1 u^\star \left[K_2^- * \cdot - K_1^+ * \cdot\right] \\ [\mathcal{L}_0]_{2,1} & [\mathcal{L}_0]_{2,2} & R_1 u^\star \left[K_2^+ * \cdot - K_1^- * \cdot\right] & -R_1 u^\star \left[K_2^- * \cdot - K_1^+ * \cdot\right] \\ R_2 v^\star K_1^- * \cdot & -R_2 v^\star K_1^+ * \cdot & -L_1 + R_2 v^\star K_1^- * \cdot & L_1 - R_2 v^\star K_1^+ * \cdot \\ -R_2 v^\star K_1^- * \cdot & R_2 v^\star K_1^+ * \cdot & L_1 - R_2 v^\star K_1^- * \cdot & -L_1 + R_2 v^\star K_1^+ * \cdot \end{bmatrix}, \tag{3.1.2}$$

with the following entries of $\mathcal{L}_0$ defined as

$$[\mathcal{L}_0]_{1,1} = -L_1 - \overline{K}_3 R_3 - R_1 u^\star \left[K_2^+ * \cdot - K_1^- * \cdot\right] \tag{3.1.3a}$$

$$[\mathcal{L}_0]_{1,2} = L_1 + \overline{K}_3 R_3 + R_1 u^\star \left[K_2^- * \cdot - K_1^+ * \cdot\right] \tag{3.1.3b}$$

$$[\mathcal{L}_0]_{2,1} = L_1 + \overline{K}_3 R_3 + R_1 u^\star \left[K_2^+ * \cdot - K_1^- * \cdot\right] \tag{3.1.3c}$$

$$[\mathcal{L}_0]_{2,2} = -L_1 - \overline{K}_3 R_3 - R_1 u^\star \left[K_2^- * \cdot - K_1^+ * \cdot\right]. \tag{3.1.3d}$$

In this form, system (3.1.1) written as an abstract linear differential equation

$$\partial_t u = \mathcal{L}(u, \mu) \tag{3.1.4}$$

with $\mu = (q_r, q_a, q_{al}) \in \mathbb{R}^3$ a vector of parameters.

3.2 Isotypic Decomposition of the Phase Space of $\mathcal{L}$

Following the general approach of Buono and Eftimie [4], we consider the domain X of the operator $\mathcal{L}$ as the phase space of (3.1.4), where X is defined as

$$X := \left\{\mathbf{u} = \left(u^+, u^-, v^+, v^-\right) \in W^{1,p}([0, L], \mathbb{R}^4) \mid \mathbf{u}^\pm(0) = \mathbf{u}^\pm(L)\right\}.$$

Since we consider a steady-state solution with isotropy subgroup $\mathbf{O(2)}$, then it follows that $\mathbf{O(2)}$ acts on X by the group actions (2.2.2) and (2.2.3), this enables us to write the *isotypic decomposition* of X. First, let $k_n = \frac{2n\pi}{L}$, and we decompose the components of $\mathbf{u} \in X$ using Fourier series decomposition [4],

$$\mathbf{u}(x) = \mathbf{a}_0^{\pm} + \mathbf{a}_1^{\pm} e^{ik_1 x} + \cdots + \mathbf{a}_n^{\pm} e^{ik_n x} + \cdots \text{c.c.},$$

where $\mathbf{a}_n^{\pm} = (a_n^+, a_n^-, b_n^+, b_n^-) \in \mathbb{C}^4$ and "c.c." stands for complex conjugates. Note that the coefficients $a_n^{\pm}, b_n^{\pm}$ are the assigned coefficients for population $u^{\pm}, v^{\pm}$, respectively. Extending Theorem 3.1 from [4], we define the following $\mathbf{O(2)}$-invariant subspaces that are isomorphic to $\mathbb{C}^4$ as

$$X_n := \left\{ \mathbf{a} e^{ik_n x} + \text{c.c.} \mid \mathbf{a} = (a^+, a^-, b^+, b^-) \in \mathbb{C}^4 \right\}. \tag{3.2.1}$$

(3.2.1) can be decomposed as $X_n = X_n^1 \oplus X_n^2 \oplus X_n^3 \oplus X_n^4$ where each $X_n^j,\ j \in \{1,2,3,4\}$ are real, four-dimensional, absolutely irreducible representations of $\mathbf{O(2)}$ and are defined as

$$\begin{aligned} X_n^1 &= \left\{ (v_0 e^{ik_n x} + \bar{v}_0 e^{-ik_n x}) f_1 \mid v_0 \in \mathbb{C} \right\}, \qquad X_n^2 = \left\{ (v_1 e^{ik_n x} + \bar{v}_1 e^{-ik_n x}) f_2 \mid v_1 \in \mathbb{C} \right\} \\ X_n^3 &= \left\{ (w_0 e^{ik_n x} + \bar{w}_0 e^{-ik_n x}) f_3 \mid w_0 \in \mathbb{C} \right\}, \quad X_n^4 = \left\{ (w_1 e^{ik_n x} + \bar{w}_1 e^{-ik_n x}) f_4 \mid w_1 \in \mathbb{C} \right\}, \end{aligned} \tag{3.2.2}$$

with $f_1 = (1,1,0,0)^T$, $f_2 = (1,-1,0,0)^T$, $f_3 = (0,0,1,1)^T$, $f_4 = (0,0,1,-1)^T$.

We show the action of $\mathbf{O(2)}$ on these absolutely irreducible subspaces as follows; Consider $\mathbf{u}_j \in X_n^j,\ j \in \{1,2,3,4\}$ then $\mathbf{u}_j = \left(u_j e^{ik_n x} + \bar{u}_j e^{-ik_n x} \right) f_j,\ u_j \in \mathbb{C}$. The action (2.2.2) on $\mathbf{u}_j \in X_n^j$ is defined as

$$\theta \cdot \mathbf{u}_j = \left(u_j e^{-ik_n \theta} e^{ik_n x} + \bar{u}_j e^{ik_n \theta} e^{-ik_n x} \right) f_j.$$

Therefore, the action of (2.2.2) on $u_j \in \mathbb{C}$ is defined as

$$\theta \cdot u_j = u_j e^{-ik_n\theta} \tag{3.2.3}$$

for $\theta \in [0, L]$. Note that, since $k_n = \frac{2n\pi}{L}$, then choosing $\theta = \frac{L}{n}$ leaves X_n^j fixed. The action (2.2.3) on $\mathbf{u}_j \in X_n^j$ is defined as

$$\kappa \cdot \mathbf{u}_j = \left(u_j e^{-ik_n x} + \bar{u}_j e^{ik_n x}\right) f_j,$$

Therefore, the action of (2.2.3) on $u_j \in \mathbb{C}$ is defined as

$$\kappa \cdot u_j = \bar{u}_j. \tag{3.2.4}$$

To make our analysis more manageable we take advantage of the absolutely irreducible representations (3.2.2) which allows for a decomposition of $\mathcal{L}$, that is,

$$\mathcal{L} = \mathcal{L}_1 \oplus \mathcal{L}_2 \oplus \cdots \oplus \mathcal{L}_n \oplus \cdots, \qquad\qquad n = 1, 2, \ldots.$$

3.2.1 Computation of $\mathcal{L}_n$

To compute $\mathcal{L}_n$ explicitly for the decomposition above, we require the following vectors

$$\mathcal{L}\left(v_0 e^{ik_n x} f_1\right), \qquad \mathcal{L}\left(v_1 e^{ik_n x} f_2\right), \qquad \mathcal{L}\left(w_0 e^{ik_n x} f_3\right), \qquad \mathcal{L}\left(w_1 e^{ik_n x} f_4\right), \tag{3.2.5}$$

where,

$$v_0 e^{ik_n x} f_1 \in X_n^1, \qquad v_1 e^{ik_n x} f_2 \in X_n^2, \qquad w_0 e^{ik_n x} f_3 \in X_n^3, \qquad w_1 e^{ik_n x} f_4 \in X_n^4 \qquad .$$

We introduce the following operators to simplify our equations

$$\overset{*}{K}{}_j^{\pm}(k_n) = \hat{K}_j^{+}(k_n) \pm \overline{\hat{K}_j^{+}(k_n)},$$

where

$$\hat{K}_j^{+}(k_n)e^{ik_nx} = K_j^{+} * e^{ik_nx} \quad \text{and} \quad \overline{\hat{K}_j^{+}(k_n)} = K_j^{-} * e^{ik_nx}.$$

Thus, giving us the following vectors

$$\mathcal{L}\left(v_0 e^{ik_nx} f_1\right) = \begin{bmatrix} -R_1u^*\left[\overset{*}{K}{}_2^{-}(k_n) + \overset{*}{K}{}_1^{-}(k_n)\right] - \gamma i k_n \\ R_1u^*\left[\overset{*}{K}{}_2^{-}(k_n) + \overset{*}{K}{}_1^{-}(k_n)\right] + \gamma i k_n \\ -R_2v^*\overset{*}{K}{}_1^{-}(k_n) \\ R_2v^*\overset{*}{K}{}_1^{-}(k_n) \end{bmatrix} v_0 e^{ik_nx}, \tag{3.2.6a}$$

$$\mathcal{L}\left(v_1 e^{ik_nx} f_2\right) = \begin{bmatrix} -R_1u^*\left[\overset{*}{K}{}_2^{+}(k_n) - \overset{*}{K}{}_1^{+}(k_n)\right] - 2L_1 - 2\overline{K}_3R_3 - \gamma i k_n \\ R_1u^*\left[\overset{*}{K}{}_2^{+}(k_n) - \overset{*}{K}{}_1^{+}(k_n)\right] + 2L_1 + 2\overline{K}_3R_3 - \gamma i k_n \\ R_2v^*\overset{*}{K}{}_1^{+}(k_n) \\ -R_2v^*\overset{*}{K}{}_1^{+}(k_n) \end{bmatrix} v_1 e^{ik_nx}, \tag{3.2.6b}$$

and

$$\mathcal{L}\left(w_0 e^{ik_n x} f_3\right) = \begin{bmatrix} -R_1 u^* \left[\overset{*}{K}_2^-(k_n) + \overset{*}{K}_1^-(k_n)\right] \\ R_1 u^* \left[\overset{*}{K}_2^-(k_n) + \overset{*}{K}_1^-(k_n)\right] \\ -R_2 v^* \overset{*}{K}_1^-(k_n) - \gamma i k_n \\ R_2 v^* \overset{*}{K}_1^-(k_n) + \gamma i k_n \end{bmatrix} w_0 e^{ik_n x}, \tag{3.2.7a}$$

$$\mathcal{L}\left(w_1 e^{ik_n x} f_4\right) = \begin{bmatrix} -R_1 u^* \left[\overset{*}{K}_2^+(k_n) - \overset{*}{K}_1^+(k_n)\right] \\ R_1 u^* \left[\overset{*}{K}_2^+(k_n) - \overset{*}{K}_1^+(k_n)\right] \\ R_2 v^* \overset{*}{K}_1^+(k_n) - 2L_1 - \gamma i k_n \\ -R_2 v^* \overset{*}{K}_1^+(k_n) + 2L_1 - \gamma i k_n \end{bmatrix} w_1 e^{ik_n x}. \tag{3.2.7b}$$

Writing (3.2.6a – 3.2.7b) in the basis of $\left\{f_j e^{ik_n x}\right\}$ gives

$$\mathcal{L}\left(v_0 e^{ik_n x} f_1\right) = \left[\left(-R_1 u^* \left[\overset{*}{K}_2^-(k_n) + \overset{*}{K}_1^-(k_n)\right] - \gamma i k_n\right) f_2 - R_2 v^* \overset{*}{K}_1^-(k_n) f_4\right] v_0 e^{ik_n x}, \tag{3.2.8a}$$

$$\begin{aligned} \mathcal{L}\left(v_1 e^{ik_n x} f_2\right) = &\left[-(\gamma i k_n) f_1 - \left(R_1 u^* \left[\overset{*}{K}_2^+(k_n) - \overset{*}{K}_1^+(k_n)\right] + 2L_1 + 2\overline{K}_3 R_3\right) f_2\right] v_1 e^{ik_n x} \\ &+ \left(R_2 v^* \overset{*}{K}_1^+(k_n) f_4\right) v_1 e^{ik_n x}, \end{aligned} \tag{3.2.8b}$$

$$\mathcal{L}\left(w_0 e^{ik_n x} f_3\right) = \left[-R_1 u^* \left[\overset{*}{K}_2^-(k_n) + \overset{*}{K}_1^-(k_n)\right] f_2 - \left(R_2 v^* \overset{*}{K}_1^-(k_n) + \gamma i k_n\right) f_4\right] w_0 e^{ik_n x}, \tag{3.2.8c}$$

$$\begin{aligned} \mathcal{L}\left(w_1 e^{ik_n x} f_4\right) = &\left[-R_1 u^* \left[\overset{*}{K}_2^+(k_n) - \overset{*}{K}_1^+(k_n)\right] f_2 - (\gamma i k_n) f_3\right. \\ &\left. + \left(R_2 v^* \overset{*}{K}_1^+(k_n) + -2L_1\right) f_4\right] w_1 e^{ik_n x}. \end{aligned} \tag{3.2.8d}$$

Writing system (3.2.8a) in matrix form, gives the 4×4 matrix

$$\mathcal{L}_n = \begin{bmatrix} 0 & -\gamma i k_n & 0 & 0 \\ [\mathcal{L}_n]_{2,1} & [\mathcal{L}_n]_{2,2} & [\mathcal{L}_n]_{2,3} & [\mathcal{L}_n]_{2,4} \\ 0 & 0 & 0 & -\gamma i k_n \\ -R_2 v^\star \overset{*}{K}_1^-(k_n) & R_2 v^\star \overset{*}{K}_1^+(k_n) & -R_2 v^\star \overset{*}{K}_1^-(k_n) - \gamma i k_n & R_2 v^\star \overset{*}{K}_1^+(k_n) - 2L_1 \end{bmatrix}, \tag{3.2.9}$$

with the entries of $\mathcal{L}_n$ defined as

$$\begin{aligned} [\mathcal{L}_n]_{2,1} &= -R_1 u^\star \left[\overset{*}{K}_2^-(k_n) + \overset{*}{K}_1^-(k_n) \right] - \gamma i k_n, \\ [\mathcal{L}_n]_{2,2} &= -R_1 u^\star \left[\overset{*}{K}_2^+(k_n) - \overset{*}{K}_1^+(k_n) \right] - 2L_1 - 2\overline{K}_3 R_3, \\ [\mathcal{L}_n]_{2,3} &= -R_1 u^\star \left[\overset{*}{K}_2^-(k_n) + \overset{*}{K}_1^-(k_n) \right], \\ [\mathcal{L}_n]_{2,4} &= -R_1 u^\star \left[\overset{*}{K}_2^+(k_n) - \overset{*}{K}_1^+(k_n) \right]. \end{aligned} \tag{3.2.10}$$

We note that, the first diagonal 2×2 block of matrix (3.2.9) corresponds to the $\mathcal{L}_n$ matrix of the one-population **M**3 model. While the second diagonal 2×2 block of matrix (3.2.9) corresponds to the $\mathcal{L}_n$ matrix of the one-population **M**4 model [4].

3.3 Critical Eigenvalues of $\mathcal{L}_n$

After computing $\mathcal{L}_n$, we now look for conditions such that $\mathcal{L}_n$ guarantees zero and purely imaginary eigenvalues. To simplify the calculations, let $\widetilde{R_1} = R_1 u^*$ and $\widetilde{R_2} = R_2 v^*$ and recall that $\overset{*}{K}_j^{\pm}(k_n) = \hat{K}_j^+(k_n) \pm \overline{\hat{K}_j^+(k_n)}$ for $j = 1, 2$ where $\hat{K}_j^+(k_n) e^{ik_n x} = K_j^+ * e^{ik_n x}$ and

Real-Valued Expressions	**Complex-Valued Expressions**
$\alpha = -\widetilde{R_1}\left[\overset{*}{K_2^+}(k_n) - \overset{*}{K_1^+}(k_n)\right] - 2L_1 - 2R_3\overline{K}_3$	$-i\eta = -\widetilde{R_1}\left[\overset{*}{K_2^-}(k_n) + \overset{*}{K_1^-}(k_n)\right]$
$\beta = \widetilde{R_2}\overset{*}{K_1^+}(k_n)$	$-i\tau = -\widetilde{R_2}\overset{*}{K_1^-}(k_n) - \gamma i k_n$
$\delta = \widetilde{R_2}\overset{*}{K_1^+}(k_n) - 2L_1$	$-i\phi = -\widetilde{R_2}\overset{*}{K_1^-}(k_n)$
$\sigma = -\widetilde{R_1}\left[\overset{*}{K_2^+}(k_n) - \overset{*}{K_1^+}(k_n)\right]$	$-i\theta = -\widetilde{R_1}\left[\overset{*}{K_2^-}(k_n) + \overset{*}{K_1^-}(k_n)\right] - \gamma i k_n$

Table 3.1: Notation used to help simplify the calculations to find the conditions such that $\mathcal{L}_n$ admits zero and purely imaginary eigenvalues. There are four real-valued functions and complex-valued functions each. In particular, $\overset{*}{K_j^+}(k_n),\ j = 1, 2$, are real-valued functions while $\overset{*}{K_j^-}(k_n),\ j = 1, 2$, are complex-valued functions.

$\overline{\hat{K}_j^+(k_n)} = K_j^- * e^{ik_n x}$, using Euler's formula we obtain the following;

$$\overset{*}{K_j^+}(k_n) = 2\int_0^\infty K_j(s)\cos(k_n s)\,\mathrm{d}s, \quad \overset{*}{K_j^-}(k_n) = 2i\int_0^\infty K_j(s)\sin(k_n s)\,\mathrm{d}s, \quad j = 1, 2. \tag{3.3.1}$$

We use the notation from Table 3.1 to rewrite the entries of $\mathcal{L}_n$ as follows

$$\mathcal{L}_n = \begin{bmatrix} 0 & -\gamma i k_n & 0 & 0 \\ -i\theta & \alpha & -i\eta & \sigma \\ 0 & 0 & 0 & -\gamma i k_n \\ -i\phi & \beta & -i\tau & \delta \end{bmatrix}. \tag{3.3.2}$$

We start with the case where $\det(\mathcal{L}_n) = 0$ which implies the condition for the zero eigenvalues of $\mathcal{L}_n$, that is;

$$\det(\mathcal{L}_n) = -(\gamma k_n)^2(\phi\eta - \theta\tau) = 0. \tag{3.3.3}$$

Since $\tau = \phi + \gamma k_n$ and $\theta = \eta + \gamma k_n$ then Eq. (3.3.3) can be expressed as

$$\eta + \phi = -\gamma k_n,$$

which can be expanded as

$$\begin{aligned} &4\widetilde{R_1}\int_0^\infty [q_r K_r(s)\sin(k_n s) - q_a K_a(s)\sin(k_n s)\ \mathrm{d}s] + \\ &2\widetilde{R_2}\int_0^\infty [q_r K_r(s)\sin(k_n s) - q_a K_a(s)\sin(k_n s) + q_{al} K_{al}(s)\sin(k_n s)\ \mathrm{d}s] = -\gamma k_n. \end{aligned} \tag{3.3.4}$$

Rearranging Eq. (3.3.4) and setting $\widetilde{R} = \left(2\widetilde{R_1} + \widetilde{R_2}\right)$ allows us to express the parameter q_r as a function of q_a and q_{al} which gives us the conditions on q_r that lead to the zero eigenvalues of $\mathcal{L}_n$to be

$$\begin{aligned} \left(2\widetilde{R}\int_0^\infty K_r(s)\sin(k_n s)\,\mathrm{d}s\right) q_r = -\gamma k_n + \left(2\widetilde{R}\int_0^\infty K_a(s)\sin(k_n s)\,\mathrm{d}s\right) q_a \\ - \left(\widetilde{R_2}\int_0^\infty K_{al}(s)\sin(k_n s)\,\mathrm{d}s\right) q_{al}. \end{aligned} \tag{3.3.5}$$

Note that Eq. (3.3.5) is a linear function of q_a and q_{al}. Therefore, the points (q_a, q_r) of Eq. (3.3.5) together with the prescribed value of q_{al} make up the conditions for $\mathcal{L}_n$ to admit zero eigenvalues for $n \in \mathbb{N}$.

In the following we consider $q_{al} = 0$ and compute $\ker(\mathcal{L}_n)$. We note that when $q_{al} = 0$, $K_1(s) = K_2(s)$ which implies $\overset{*}{K_2^-}(k_n) = \overset{*}{K_1^-}(k_n)$ and $\overset{*}{K_2^+}(k_n) = \overset{*}{K_1^+}(k_n)$. Equation (3.3.4) then simplifies to $-\gamma i k_n = \widetilde{R}\overset{*}{K_2^-}(k_n)$ and since $\widetilde{R} - 2\widetilde{R_1} = \widetilde{R_2}$, $\widetilde{R} - 2\widetilde{R_2} = \widetilde{R_1}$ then

matrix (3.2.9) can be expressed as

$$\mathcal{L}_n = \begin{bmatrix} 0 & \widetilde{R}\overset{*}{K}_2^-(k_n) & 0 & 0 \\ \widetilde{R_2}\overset{*}{K}_2^-(k_n) & -2\left[L_1 + R_3\overline{K}_3\right] & -2\widetilde{R_1}\overset{*}{K}_2^-(k_n) & 0 \\ 0 & 0 & 0 & \widetilde{R}\overset{*}{K}_2^-(k_n) \\ -\widetilde{R_2}\overset{*}{K}_2^-(k_n) & \widetilde{R_2}\overset{*}{K}_2^+(k_n) & 2\widetilde{R_1}\overset{*}{K}_2^-(k_n) & \widetilde{R_2}\overset{*}{K}_2^+(k_n) - 2L_1 \end{bmatrix}. \tag{3.3.6}$$

Using a row-reduction method on matrix (3.3.6) we obtain the basis of the eigenspace corresponding to the zero eigenvalue which is

$$\mathbf{v} = (1, 0, 1, 0)^T. \tag{3.3.7}$$

In other words, $\ker(\mathcal{L}_n) = \text{span}\left\{e^{ik_n x}\mathbf{v}\right\} \neq \{0\}$.

Next, we find conditions such that $\mathcal{L}_n$ admits purely imaginary eigenvalues. That is, we solve for ω such that $\det(\mathcal{L}_n - i\omega I_4) = 0$, where I_4 is a 4×4 identity matrix. Using the expressions from Table 3.1, we solve $\det(\mathcal{L}_n - i\omega I_4) = 0$ as follows; Starting from a cofactor expansion along the first row of $\mathcal{L}_n - i\omega I_4$, we obtain

$$\begin{aligned} \det(\mathcal{L}_n - i\omega I_4) = \omega^2 \begin{vmatrix} \alpha - i\omega & \sigma \\ \beta & \delta - i\omega \end{vmatrix} + \omega\gamma k_n \begin{vmatrix} \alpha - i\omega & -i\eta \\ \beta & -i\tau \end{vmatrix} + \\ \omega\gamma k_n \begin{vmatrix} -i\theta & \sigma \\ -i\phi & \delta - i\omega \end{vmatrix} + \gamma^2 k_n^2 \begin{vmatrix} -i\theta & -i\eta \\ -i\phi & -i\tau \end{vmatrix} = 0. \end{aligned} \tag{3.3.8}$$

The 2×2 determinants in Eq. (3.3.8) can then be expanded. After grouping the real and

complex parts together we find

$$\underbrace{\omega^4 - (\alpha\delta - \sigma\beta + \gamma k_n(\tau+\theta))\,\omega^2 - (\phi\eta - \theta\tau)\,(\gamma k_n)^2}_{\text{Real Part}} \; + \tag{3.3.9}$$

$$i\underbrace{\left[(\alpha+\delta)\,\omega^3 - (\alpha\tau - \eta\beta + \theta\delta - \phi\sigma)\,\gamma k_n \omega\right]}_{\text{Imaginary Part}} \;=\; 0.$$

For Eq. (3.3.9) to be satisfied, its real and imaginary parts must vanish. Thus, we perform a two-stage approach to find conditions so that $\mathcal{L}_n$ admits purely imaginary eigenvalues. First, we set the imaginary part of (3.3.9) to zero and solve for ω so that

$$(\alpha+\delta)\,\omega^3 - (\alpha\tau - \eta\beta + \theta\delta - \phi\sigma)\,\gamma k_n \omega = 0.$$

Ignoring the trivial solution gives

$$\omega = \pm\left[\frac{(\alpha\tau + \theta\delta - (\eta\beta + \phi\sigma))\gamma k_n}{\alpha+\delta}\right]^{1/2}. \tag{3.3.10}$$

Second, we replace the ω from the real part of (3.3.9) with the solution (3.3.10)

$$\frac{1}{(\alpha+\delta)^2}\left(\alpha\tau + \theta\delta - (\beta\eta + \phi\sigma)\right)^2 (\gamma k_n)^2 -$$

$$\frac{1}{\alpha+\delta}\left(\alpha\delta - \sigma\beta + \gamma k_n(\tau+\theta)\right)\left(\alpha\tau + \theta\delta - (\beta\eta + \phi\sigma)\right)(\gamma k_n) - (\phi\eta - \theta\tau)\,(\gamma k_n)^2 \;= 0,$$

which leads to the following equation

$$\left(\alpha\tau + \theta\delta - (\beta\eta + \phi\sigma)\right)^2 -$$

$$\frac{1}{\gamma k_n}\left(\alpha\delta - \sigma\beta + (\gamma k_n)(\tau+\theta)\right)\left(\alpha\tau + \delta\theta - (\beta\eta + \phi\sigma)\right)(\alpha+\delta) - (\phi\eta - \theta\tau)\,(\alpha+\delta)^2 = 0. \tag{3.3.11}$$

Equation (3.3.11) allows us to determine the conditions on the parameters $q_j,\ j = \{r, a, al\}$ so that $\mathcal{L}_n$ admits purely imaginary eigenvalues.

Figure 3.1 shows the neutral stability curves obtained from `MATLAB` computations that solves Eq. (3.3.11) for q_r. The dashed curves represent the values of (q_r, q_a) such that $\mathcal{L}_n$ admits zero eigenvalues and the solid curves represent the conditions on (q_r, q_a) such that $\mathcal{L}_n$ admits purely imaginary eigenvalues. We note that, the region of asymptotic stability from Figure 3.1 applies only to wave numbers up to $n = 6$. A proof of the convergence or divergence of the bounded region of asymptotic stability is an avenue for future research. In particular, we have only shown the region for asymptotic stability for small k_n value without considering the case as $k_n \to \infty$, will the neutral stability curves converge to some shape to form a boundary or will the curves diverge as k_n becomes large? As (q_a, q_r) varies and one of the solid curves are crossed, spontaneous symmetry-breaking occurs as an eigenvalue crosses the imaginary axis with nonzero imaginary part, this corresponds to a Hopf bifurcation. Symmetry-breaking at a steady-state bifurcation is also possible, in particular, it occurs as (q_a, q_r) are varied such that the dashed curves are crossed. It is easy to see from Fig. 3.1 that crossing the steady-state curves lead to unstable nonhomogeneous solutions because for the values of (q_r, q_a) that correspond to these steady-state curves, the fully-symmetric equilibrium solution has already become unstable and thus, unstable solutions have to branch off from it. We also highlight the existence of codimension-two bifurcation points at the intersection points of curves, where the intersection of purely imaginary eigenvalue curves with different wave numbers lead to Hopf/Hopf codimension-two points and the intersection of zero and purely imaginary eigenvalue curves lead to steady-state/Hopf codimension-two points. Generically, these points are not crossed in one-parameter families and thus codimension-two bifurcation points are not further discussed in this thesis.

`MATLAB` computations also show that the eigenvectors $\mathbf{v}_1, \mathbf{v}_2$ corresponding to the pair

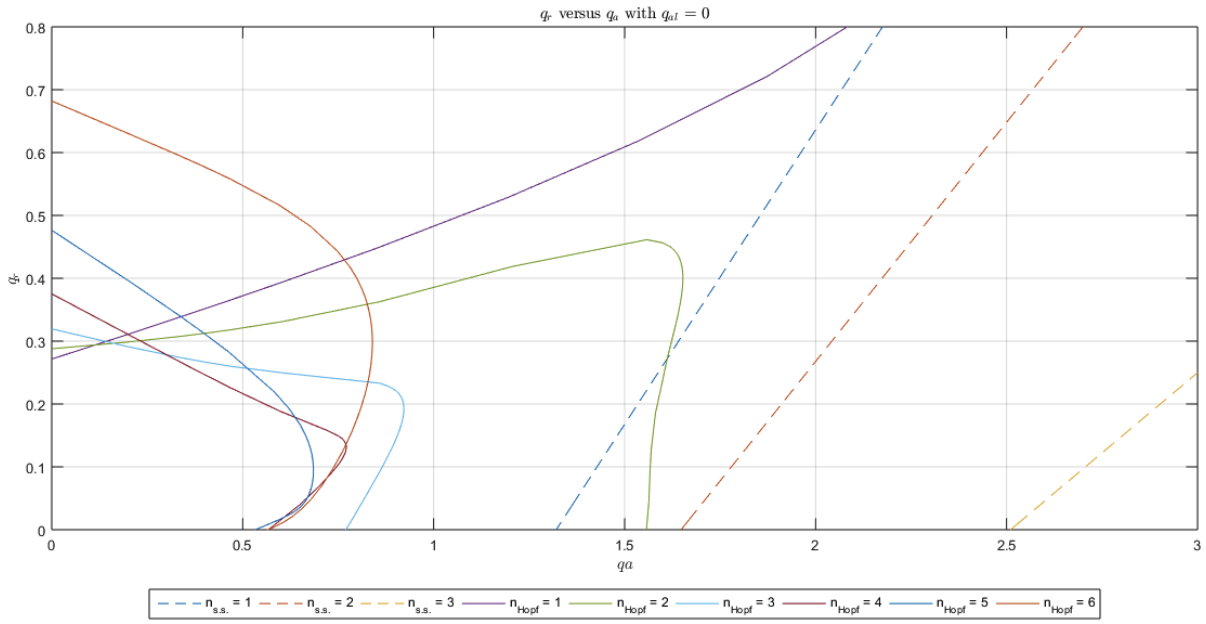

Figure 3.1: Neutral stability curves generated from MATLAB which determines the values of q_r and q_a such that $\mathcal{L}_n$ admits zero and purely imaginary eigenvalues. The dashed lines represent the curves for the zero eigenvalues and the solid lines represent the curves for the purely imaginary eigenvalues. The wave number n corresponds to k_n which will determine the isotropy subgroup of the solutions at bifurcation.

of purely imaginary eigenvalues $\pm i\omega$ are of the following form

$$\mathbf{v}_1 = \begin{bmatrix} a_1 + ib_1 \\ a_2 + ib_2 \\ c_1 \\ c_2 \end{bmatrix}, \qquad \mathbf{v}_2 = \begin{bmatrix} -a_1 + ib_1 \\ a_2 - ib_2 \\ -c_1 \\ c_2 \end{bmatrix} \tag{3.3.12}$$

with $a_k, b_k, c_k \in \mathbb{R}$, $k = 1, 2$. Since $\mathcal{L}_n$ is written in terms of the basis vectors $f_1 = (1, 1, 0, 0)^T$, $f_2 = (1, -1, 0, 0)^T$, $f_3 = (0, 0, 1, 1)^T$, $f_4 = (0, 0, 1, -1)^T$ we can then write the eigenvectors (3.3.12) as

$$\begin{aligned} \mathbf{v}_1 &= (a_1 + ib_1)\, f_1 + (a_2 + ib_2)\, f_2 + c_1 f_3 + c_2 f_4 \\ \mathbf{v}_2 &= -\overline{(a_1 + ib_1)} f_1 + \overline{(a_2 + ib_2)} f_2 - c_1 f_3 + c_2 f_4. \end{aligned} \tag{3.3.13}$$

Equation (3.3.13) allows us to define the eigenspace of purely imaginary eigenvalues inside

the space $\mathcal{L}_n$ by including the spatial parts $e^{\pm ik_n x}$, i.e.,

$$h_1^n = e^{ik_n x}\mathbf{v}_1, \qquad\qquad h_2^n = -e^{-ik_n x}\overline{\mathbf{v}}_2. \tag{3.3.14}$$

Where we claim the action of $\mathbf{O(2)}$ on (h_1^n, h_2^n) via (2.2.2) and (2.2.3) are as follows;

$$\theta \cdot (h_1^n, h_2^n) = \left(e^{-ik_n\theta}h_1^n, e^{ik_n\theta}h_2^n\right), \qquad\qquad \kappa \cdot (h_1^n, h_2^n) = (h_2^n, h_1^n). \tag{3.3.15}$$

To prove this claim, consider the actions (2.2.2) and (2.2.3) on (h_1, h_2)

$$\theta \cdot h_1^n = e^{ik_n(x-\theta)}\mathbf{v}_1 = e^{-ik_n\theta}h_1^n \qquad \theta \cdot h_2^n = -e^{-ik_n(x+\theta)}\overline{\mathbf{v}}_2 = e^{ik_n\theta}h_2^n. \tag{3.3.16}$$

Since $\kappa \cdot f_{1,3} = f_{1,3}$ and $\kappa \cdot f_{2,4} = -f_{2,4}$ then we have

$$\begin{aligned} \kappa \cdot h_1^n &= e^{ik_n x}\left((a_1 + ib_1)\, f_1 + (a_2 + ib_2)\, f_2 + c_1 f_3 + c_2 f_4\right) \\ &= e^{-ik_n x}\left((a_1 + ib_1)\, f_1 - (a_2 + ib_2)\, f_2 + c_1 f_3 - c_2 f_4\right) = -e^{-ik_n x}\overline{\mathbf{v}}_2 = h_2^n, \end{aligned}$$

thus we prove $\kappa \cdot (h_1^n, h_2^n) = (h_2^n, h_1^n)$.

Chapter 4

Symmetry-Breaking Bifurcations of Equilibria

In this chapter we study the structure of bifurcations of the spatially homogeneous steady-state solutions (2.3.2) of the system (2.1.1). It is shown in Chapter 3 that there exist values for the parameters (q_r, q_a) with $q_{al} = 0$ such that the linear operator $\mathcal{L}_n$ admit critical eigenvalues, which then lead to the existence of branches of bifurcating solutions due to steady-state and Hopf bifurcations. In particular, we consider these bifurcations under the presence of the $\mathbf{O(2)}$ symmetry. This chapter is organized as follows; In Section 4.1 we discuss symmetry-breaking of (2.3.2) at steady-state bifurcation, the *Equivariant Branching Lemma* is then applied to determine the symmetry of the bifurcating branches that emanate from the bifurcation point. In Section 4.2 we discuss symmetry-breaking at Hopf bifurcation and apply the analog to the Equivariant Branching Lemma for periodic solutions, the *Equivariant Hopf Theorem* [19]. The Equivariant Hopf Theorem forces us to consider *spatio-temporal* symmetries so that we can capture all bifurcating branches of periodic solutions emanating from the bifurcation point [18, 19]. In Section 4.3, we generate plots for the eigenfunctions corresponding to the bifurcating solutions from both steady-state and Hopf bifurcations. A classification of these solutions based on their isotropy

subgroups are also shown and discussed. A generic description of the Liapunov-Schmidt reduction as described by Golubitsky and Schaeffer [17] is given in Section 4.4. Lastly a discussion on the general form of the $\mathbf{O(2)}$-equivariant and $\mathbf{O(2)} \times \mathbf{S^1}$-equivariant mappings is shown in Section 4.5 in order to determine the criticality and stability of the bifurcating solutions.

4.1 Symmetry-Breaking in Steady-State Bifurcation

In this section we study the structure of bifurcations of the homogeneous steady-state solution $\mathbf{u}_0 = (u^+, u^-, v^+, v^-) = (A_u/2, A_u/2, A_v/2, A_v/2)$ of the system (2.1.1). Recall that this steady-state solution has the isotropy subgroup $\Sigma_{\mathbf{u}_0} = \mathbf{O(2)}$, given this isotropy subgroup, it follows that $\mathbf{u}_0 \in \mathrm{Fix}\,(\mathbf{O(2)})$. Our goal is to determine the class of solutions that appear once $\mathbf{u}_0$ undergoes a steady-state bifurcation, as previously mentioned we use the *Equivariant Branching Lemma* to answer this problem. Given a general Γ-equivariant system $\partial_t = F(\mathbf{u}, \lambda)$, we describe the generic conditions for steady-state bifurcations to occur: The main one being $V = \ker(dF)_{0,\lambda_0}$ is nonzero and it is an *absolutely irreducible representation of* ***O(2)***. Absolutely irreducible representations of the group Γ are defined as follows;

Definition 4.1.1. *A representation of a group Γ on a space V is absolutely irreducible if the only linear mappings on V that commute with Γ are scalar multiples of identity.*

Next we show the Equivariant Branching Lemma as described by Golubitsky et al. [19];

Theorem 4.1.2 (Equivariant Branching Lemma)**.** *Let Γ be a compact Lie group acting on some vector space V.*

(a) Let $F : V \times \mathbb{R} \to V$ be Γ-equivariant.

(b) Without loss of generality, let $x^\star = 0$ *be a steady-state solution for all parameter values. Assumptions (a) and (b) imply:*

$$F(0,\lambda) \equiv 0,$$
$$(dF)_{0,\lambda} = c(\lambda)\, I.$$

(c) Where $c : \mathbb{R} \to \mathbb{R}$ *such that;*

- $c(0) = 0$ *(condition for a bifurcation to occur).*
- $\frac{\mathrm{d}}{\mathrm{d}\lambda} c(0) \neq 0$ *(eigenvalue crossing condition).*

(d) If there exist an axial subgroup $\Sigma \subset \Gamma$ *(i.e.,* $dim\,(Fix\,\Sigma) = 1$*).*

Then there exists a unique branch of solutions to $F(x,\lambda) = 0$ *emanating from* $(0,0)$ *where the symmetry of the solutions is* Σ*.*

To apply Theorem (4.1.2), we rewrite (2.1.1) as

$$\partial_t \mathbf{u} = F[\mathbf{u}, \mu] \tag{4.1.1}$$

where $\mathbf{u} = (u^+(x,t), u^-(x,t), v^+(x,t), v^-(x,t))$ and μ is a vector of parameters i.e., $\mu = (q_r, q_a, q_{al})$. We have previously shown that system (4.1.1) is $\mathbf{O(2)}$-equivariant with

$$F(\mathbf{u}_0, \mu) \equiv 0 \tag{4.1.2}$$

and $\mathcal{L} = \partial_{\mathbf{u}} F(\mathbf{u}_0, \mu)$. In particular, if we consider the decomposition $\mathcal{L}_n$ of $\mathcal{L}$ where $\mathcal{L}_n$ has a zero eigenvalue then it follows that $V := \ker(\mathcal{L}_n)$ where $\ker(\mathcal{L}_n)$ is of the form (3.3.7). $\mathbf{O(2)}$ acts absolutely irreducibly on the subspace $V = \text{span}\left\{e^{ik_n x}\,(1,0,1,0)^T\right\}$ via (2.2.2) and (2.2.3) as follows; First the translation action (2.2.2) applied to V returns

$$\theta \cdot \left(e^{ik_n x}\,(1,0,1,0)^T\right) = e^{ik_n(x-\theta)}\,(1,0,1,0)^T = e^{-ik_n\theta}\left(e^{ik_n x}\,(1,0,1,0)^T\right).$$

Therefore the action of (2.2.2) on $v \in V$ is defined as

$$\theta \cdot v = e^{-ik_n\theta} v \tag{4.1.3}$$

for $\theta \in [0, L]$. Since $k_n = \frac{2n\pi}{L}$, if we choose $\theta = \frac{L}{n}$ then V is fixed by θ. Next, the reflection action (2.2.3) applied to V returns

$$\kappa \cdot \left(e^{ik_n x} (1, 0, 1, 0)^T \right) = e^{ik_n(L-x)} (1, 0, 1, 0)^T = e^{-ik_n x} (1, 0, 1, 0)^T .$$

Therefore, the action of (2.2.3) on $v \in V$ is defined as

$$\kappa \cdot v = \overline{v}. \tag{4.1.4}$$

Notice that v is fixed by κ if and only if $\mathrm{Im}(v) = 0$. That is,

$$\mathrm{Fix}\left(\mathbb{Z}_2(\kappa)\right) = \{v \in \mathbb{C} \mid \mathrm{Im}(v) = 0\} = \mathbb{R}.$$

The similarity of the action of $\mathbf{O(2)}$ on (3.2.3 – 3.2.4) and (4.1.3 – 4.1.4) implies that $V \simeq X_n^j$, thus, V is an absolutely irreducible representation. Recall from Chapter 1.1, the group of symmetries denoted by $\mathbf{D}_n = \left\langle \frac{L}{n}, \kappa \right\rangle$ called *Dihedral group of order* $2n$. Notice that

$$\mathrm{Fix}\left(\mathbf{D}_n\right) = \mathrm{Fix}\left(\mathbb{Z}_2(\kappa)\right) = \mathbb{R}.$$

Therefore, given the conditions above, we have just determined a subgroup $\Sigma \subset \mathbf{O(2)}$ such that Σ is an axial isotropy subgroup (i.e., dim $\mathrm{Fix}\left(\mathbf{D}_n\right) = 1$). We point out that, $\mathbf{D}_n$ is not the only axial subgroup, but there are conjugate axial isotropy subgroups generated by $\left\langle \frac{L}{n}, \theta^{-1}\kappa\theta \right\rangle$, $\forall \theta \in [0, L]$. This result is summarized in the following statement:

Theorem 4.1.3. *Let* $(\boldsymbol{u}_0, \mu_0)$ *be an equilibrium point of the system*

$$F(\boldsymbol{u}, \mu),$$

with $F : X \times \mathbb{R}^p \to X$ *and* $\mathcal{L} = (dF)_{\boldsymbol{u}_0,\mu_0}$ *with* $V = ker\,\mathcal{L} \neq 0$ *and is an absolutely irreducible representation of* ***O(2)****. Then given the actions (2.2.2) and (2.2.3) on* V*, where* $\theta = \frac{L}{n}$ *it follows that* $\boldsymbol{D}_n\langle\frac{L}{n}, \kappa\rangle \subset$ ***O(2)*** *is an axial isotropy subgroup. We note that there also exist conjugate isotropy subgroups* $\boldsymbol{D}_n\langle\frac{L}{n}, \theta^{-1}\kappa\theta\rangle$ *with a one-dimensional fixed-point subspace. Therefore, by the Equivariant branching lemma, there exists a branch of nonhomogeneous steady-state solutions with* $\boldsymbol{D}_n < \frac{L}{n}, \kappa >$*-symmetry with an* ***SO(2)*** *group orbit of solutions with isotropy subgroup* $\boldsymbol{D}_n < \frac{L}{n}, \theta^{-1}\kappa\theta >$ *that emanates from the homogeneous steady-state* $(\boldsymbol{u}_0, \mu_0)$*.*

4.2 Symmetry-Breaking in Hopf Bifurcation

It is shown in Chapter 3 that Eq. (3.3.11) determines the conditions for the existence of purely imaginary eigenvalues of the linear operator $\mathcal{L}_n$ which implies the occurrence of a Hopf bifurcation. However the $\mathbf{O(2)}$-symmetry that the system possesses can force the system to have multiple eigenvalues because the action of $\mathbf{O(2)}$ on $\mathbb{C} \simeq \mathbb{R}^2$ is absolutely irreducible, therefore the standard Hopf theorem does not apply directly [19]. In this section, we show the existence of a branch of periodic solutions subject to the conditions of the *Equivariant Hopf Theorem* [19]. As a counterpart absolutely irreducible representations, we define conditions on the action of Γ that allow $(df)_{0,\lambda}$ to have purely imaginary eigenvalues, namely, Γ-*simple representations*;

Definition 4.2.1. *A representation* W *of a compact Lie group* Γ *is* Γ*-simple if either*

(a) $W \simeq V \oplus V$ *is absolutely irreducible for* Γ*, or*

(b) W is non-absolutely irreducible for Γ.

First, we note that if $W = V$ then by absolute irreducibility the Γ-equivariant linear map is of the form

$$J = c(\lambda)I,\ c \in \mathbb{R}$$

which returns real (repeated) eigenvalues, which implies that Hopf bifurcation cannot occur. Note that we can not have the form W non-absolutely irreducible because $\mathbf{O(2)}$ only has absolutely irreducible representations [19]. Therefore, in the following we only consider Γ-simple representations of the form $W = V \oplus V$ where V is an absolutely irreducible representation. To show this, consider a linear map $L : W \to W$ that is Γ-equivariant where $W = V \oplus V$ with V an absolutely irreducible representation, then L expressed in block matrix form is

$$L = \begin{bmatrix} A & B \\ C & D \end{bmatrix}$$

with A, B, C, D are of the form

$$A = aI, B = bI, \ldots, D = dI,\ \{a, b, c, d\} \in \mathbb{R}.$$

The characteristic polynomial of L is

$$\det\left(L - \mu I\right) = \left[\left(a - \mu\right)\left(d - \mu\right) - bc\right]^m. \tag{4.2.1}$$

To obtain purely imaginary eigenvalues we set $a + d = 0, ad - bc = 1$ and finally to obtain the normal form of

$$(dF)_{0,\lambda_0} = \begin{bmatrix} 0 & -I \\ I & 0 \end{bmatrix} \tag{4.2.2}$$

as described in [19], we use a rotation matrix so that $a = d = 0,\ b = -1, c = 1$.

When symmetry is present it is imperative to consider both *temporal and spatial* sym-

metries for one to be able to detect all branches of periodic solutions at a Hopf bifurcation with symmetry Γ. As before, the spatial symmetries of our system come from $\Gamma = \mathbf{O(2)}$ and the temporal symmetries are phase-shifts along the periodic solution which forms the *circle group* $\mathbf{S^1}$. In particular $\mathbf{S^1}$ can be described as follows; Without loss of generality, we assume that $v(t)$ is a 2π-periodic solution, since the PDE (2.1.1) is autonomous then it is invariant with respect to any phase-shifts. Therefore, for any 2π-periodic solution $v(t)$ all phase-shifts $[0, 2\pi)$ leave the periodic solution invariant. The existence of Γ-simple representations lead to the analogies between steady-state bifurcation and Hopf bifurcation with symmetry, in which Γ is replaced by $\Gamma \times \mathbf{S^1}$ [19]. To describe the symmetry of a 2π-periodic function $v(t)$, we identify $\mathbf{S^1}$ with $\mathbb{R}/2\pi\mathbb{Z}$. Then a symmetry of a periodic function $v(t)$ is an element $(\gamma, \theta) \in \Gamma \times \mathbf{S^1}$ such that

$$\gamma \cdot v(t) = v(t - \theta). \tag{4.2.3}$$

Here, (γ, θ) is a mixture of spatial and temporal symmetries. The action of $\mathbf{S^1}$ on periodic solutions is called the *phase-shift*. In a similar manner to the isotropy subgroup for the steady-state case, the collection of all symmetries for $v(t)$ forms a subgroup of $\Gamma \times \mathbf{S^1}$

$$\Sigma_{v(t)} := \{(\gamma, \theta) \in \Gamma \times \mathbf{S^1} \mid \gamma v(t) = v(t - \theta)\}. \tag{4.2.4}$$

The natural action of $\Gamma \times \mathbf{S^1}$ on the space 2π-periodic functions is defined by

$$(\gamma, \theta) \cdot v(t) = \gamma v(t + \theta). \tag{4.2.5}$$

Equation (4.2.5) allows us to rewrite (4.2.4) as

$$(\gamma, \theta) \cdot v(t) = v(t)$$

which verifies that $\Sigma_{v(t)}$ is the isotropy subgroup of $v(t)$. In the following, we introduce the Equivariant Hopf Theorem as described in [19].

Theorem 4.2.2 (Equivariant Hopf Theorem)**.** *Consider the system of PDEs*

$$\frac{\partial \boldsymbol{u}}{\partial t} = F(\boldsymbol{u}, \lambda)$$

where $F : V \times \mathbb{R} \to V$ is smooth and Γ-equivariant for some compact Lie group Γ. Assume that $F(0, \lambda_0) = 0$ and the centre subspace is Γ-simple so that $J = (dF)_{0,\lambda_0}$ is of the form

$$J = \begin{bmatrix} 0 & -I_m \\ I_m & 0 \end{bmatrix}.$$

Suppose that there exists a $\mathbb{C}$-axial subgroup Σ of $\Gamma \times \mathbf{S^1}$ (i.e., dim Fix$(\Sigma) = 2$). Then there exists a unique branch of 2π-periodic solutions, having Σ as their group of symmetries.

In Section 3.3 we introduced the basis for $\mathbb{C}^2$ (3.3.14), we now show the action of $\mathbf{O(2)}$ and $\mathbf{S^1}$ on coordinates of $\mathbb{C}^2$: (z_1, z_2);

$$\begin{aligned} \psi \cdot (z_1, z_2) &= \left(e^{i\psi} z_1, e^{i\psi} z_2\right), & \psi &\in \mathbf{S^1}, \\ \theta \cdot (z_1, z_2) &= \left(e^{-ik_n\theta} z_1, e^{ik_n\theta} z_2\right), & \theta &\in \mathbf{SO(2)}, \\ \kappa \cdot (z_1, z_2) &= (z_2, z_1), & \kappa &\in \mathbf{O(2)}. \end{aligned} \tag{4.2.6}$$

To show this claim, consider $\mathbf{u} \in \mathbb{C}^2$, that is;

$$\mathbf{u} = z_1 h_1^n + z_2 h_2^n + c.c.,$$

we recall that from (4.2.6), the action of $\mathbf{O(2)}$ on $\mathbf{u}$ is given as follows

$$\theta \cdot \mathbf{u} = z_1 e^{-ik_n\theta} h_1^n + z_2 e^{ik_n\theta} h_2^n = \left(e^{-ik_n\theta} z_1\right) h_1^n + \left(e^{ik_n\theta} z_2\right) h_2^n,$$
$$\kappa \cdot \mathbf{u} = z_1 \left(\kappa \cdot h_1^n\right) + z_2 \left(\kappa \cdot h_2^n\right) = z_2 h_2^n + z_1 h_1^n.$$

Therefore, (4.2.6) is proven.

We now investigate the isotropy subgroups of the $\mathbf{O(2)} \times \mathbf{S^1}$ action, consider the action of (θ, ψ) on (z_1, z_2), that is,

$$(\theta, \psi) \cdot (z_1, z_2) = \left(e^{-ik_n\theta} e^{i\psi} z_1, e^{ik_n\theta} e^{i\psi} z_2\right) = \left(e^{i(-k_n\theta+\psi)} z_1, e^{i(k_n\theta+\psi)} z_2\right). \tag{4.2.7}$$

We note that (θ, ψ) only fixes (z_1, z_2) if the coordinates are chosen to be

$$(z_1, z_2) = (0, b) \text{ or } (b, 0) \quad \text{for } b \in \mathbb{R}. \tag{4.2.8}$$

Condition (4.2.8) follows directly from (4.2.7). That is, if we consider $\psi = -k_n\theta$ then

$$(\theta, -k_n\theta) \cdot (z_1, z_2) = \left(e^{-2ik_n\theta} z_1, z_2\right) = (z_1, z_2),$$

which then implies that $(z_1, z_2) = (0, b)$ for $b \in \mathbb{R}$. We note that the coordinates from (4.2.8) are orbit representatives of the following isotropy subgroup

$$\widetilde{\mathbf{SO(2)}} \;:=\; \{(\theta, -k_n\theta) \;|\; \theta \in \mathbf{SO(2)}\}. \tag{4.2.9}$$

Next, we consider the action of (κ, ψ) on (z_1, z_2), that is,

$$(\kappa, \psi) \cdot (z_1, z_2) \;=\; \left(e^{i\psi} z_2, e^{i\psi} z_1\right), \tag{4.2.10}$$

if we consider $\psi = 0$, then

$$(\kappa, 0) \cdot (z_1, z_2) = (z_2, z_1)\,,$$

which implies $z_1 = z_2$. If we consider $z_1 = z_2 = b > 0$ and let (θ, ψ) act on (b, b), then,

$$(\theta, \psi) \cdot (b, b) \;\; = \;\; \left(e^{-ik_n\theta}e^{i\psi}b, e^{ik_n\theta}e^{i\psi}b\right). \tag{4.2.11}$$

Since $k_n = \frac{2n\pi}{L}$, then setting $\theta = \frac{L}{2n}$ and $\psi = \pi$ allows us to fix (b, b), that is,

$$\left(\frac{L}{2n}, \pi\right) \cdot (b, b) = (b, b)\,. \tag{4.2.12}$$

We note that the coordinates (b, b) are orbit representatives of the isotropy subgroup

$$\mathbb{Z}_2(\kappa) \times Z_{2n}\left(\frac{L}{2n}, \pi\right). \tag{4.2.13}$$

Since we are considering a temporal period of 2π, setting $\psi = \pi$ actually represents a temporal shift of half a period.

Lastly, since (4.2.9) and (4.2.13) fix coordinates of the form $(0, b)$ and (b, b), respectively, then it follows that both (4.2.9) and (4.2.13) are $\mathbb{C}$-axial subgroups of $\mathbf{O(2)} \times \mathbf{S^1}$. By the Equivariant Hopf Theorem, there exist unique branches of 2π-periodic solutions emanating from the $\mathbf{O(2)} \times \mathbf{S}^1$-symmetric steady-state with symmetries (4.2.9) and (4.2.13). This result is summarized in the following statement:

Theorem 4.2.3. *Let $(\boldsymbol{u}_0, \mu_0)$ be an equilibrium point of the $\boldsymbol{O(2)} \times \mathbf{S^1}$ system*

$$F(\boldsymbol{u}, \mu)\,,$$

with $F : X \times \mathbb{R}^p \to X$ and $\mathcal{L} = (dF)_{\boldsymbol{u}_0,\mu_0}$. Consider the $\mathbb{C}$-axial representation $W =$

$W_1^n \oplus W_2^n$ *with* $W_k^n \simeq \left\{ z_k e^{ik_n x} h_k^n + c.c \mid z_k \in \mathbb{C} \right\}$*, then it follows that* $\mathcal{L}_n$ *is of the form*

$$\mathcal{L}_n = \begin{bmatrix} 0 & -I \\ I & 0 \end{bmatrix}.$$

Given the actions (2.2.2) and (2.2.3) on the basis of $\mathbb{C}^2$ *(3.3.14), and the temporal shift induced by the group* $\boldsymbol{S^1}$*. We obtain the actions of* $\boldsymbol{O(2) \times S^1}$ *on the coordinates of* $\mathbb{C}^2$ *given by (4.2.6). The actions (4.2.6) lead to the* $\mathbb{C}$*-axial subgroups of* $\boldsymbol{O(2) \times S^1}$ *denoted as (4.2.9) and (4.2.13) which fixes coordinates of the form* $(0, b)$ *and* (b, b) *for some* $b \in \mathbb{R}$*, respectively. Therefore, by the Equivariant Hopf Theorem, the existence of branches of* 2π*-periodic solutions that emanate from the* $\boldsymbol{O(2) \times S^1}$*-symmetric homogeneous steady-states at Hopf bifurcation is proven. For which these solutions exhibit the symmetries* $\widetilde{\boldsymbol{SO(2)}}$ *and* $\mathbb{Z}_2(\kappa) \times Z_{2n}\left(\frac{L}{2n}, \pi\right)$ *that correspond to rotating wave and standing wave solutions, respectively.*

4.3 Linear Modes at Bifurcation

After showing the existence of the axial and $\mathbb{C}$-axial subgroups with the following symmetries; $\mathbf{D}_n$, $\widetilde{\mathbf{SO(2)}}$ and $\mathbb{Z}_2(\kappa) \times Z_{2n}\left(\frac{L}{2n}, \pi\right)$ which correspond to the stationary pulse (S.P.), rotating (R.W.) and standing wave (S.W.) solutions, respectively. We now calculate the linear terms of the eigenfunctions of the bifurcating solutions. Since near a bifurcation point the eigenfunctions give an approximation to the bifurcating solutions [4], we create plots for these eigenfunctions; here we choose to plot the total density $w(x,t)$ to represent the behaviour of each solution $\{u^+(x,t), u^-(x,t), v^+(x,t), v^-(x,t)\}$ to avoid showing redundant plots. These plots can then be used as a guide for classifying solutions obtained via numerical simulations. In particular, the plots can be used for identifying isotropy subgroups of numerical solutions [4].

Consider the linear system

$$\partial_t U(x,t) = \mathcal{L}_n U(x,t) \tag{4.3.1}$$

with $U(x,t) = (u^+(x,t), u^-(x,t), v^+(x,t), v^-(x,t))$. Using the basis $\{f_1, f_2, f_3, f_4\}$, the solutions can be written as

$$U(x,t) = Re\left(v_0 e^{ik_n x} e^{\sigma t}\right) f_1 + Re\left(v_1 e^{ik_n x} e^{\sigma t}\right) f_2 + Re\left(w_0 e^{ik_n x} e^{\sigma t}\right) f_3 + Re\left(w_1 e^{ik_n x} e^{\sigma t}\right) f_4. \tag{4.3.2}$$

For the eigenvalue $\sigma = 0$ the corresponding eigenspace is 1-D complex and given as $(f_1 + f_3)$, thus, the corresponding eigenfunction is

$$U(x,t) = Re\left(z_0 e^{ik_n x}\right)(f_1 + f_3). \tag{4.3.3}$$

This solution corresponds to a stationary pulse with $\mathbf{D}_n$-symmetry. In particular, this type of solution emerges once one of the dashed curves from Fig. 3.1 are crossed (i.e., $n = 1, 2, 3$) as the parameters (qa, qr) are varied. The total density $w(x,t) = u^+(x,t) + u^-(x,t) + v^+(x,t) + v^-(x,t)$ for (4.3.3) is then given as

$$w(x,t) = 4Re\left(z_0 e^{ik_n x}\right). \tag{4.3.4}$$

Figures (4.1a –4.1c) show the S.P. solutions corresponding to the wave numbers $n = 1, 2, 3$. Notice that when $n = k$ for $k = 1, 2, 3$, we see a k-bump solution that is L-periodic. These bumps can be thought of as equispaced objects around a circle each with an axis of symmetry about its vertex; hence, the $\mathbf{D}_n$-equivariance is shown for the S.P. solutions. After discussing the solutions obtained from steady-state bifurcation, we now look at solutions obtained from a Hopf bifurcation. Recall that when $\sigma = \pm i\omega t$ the

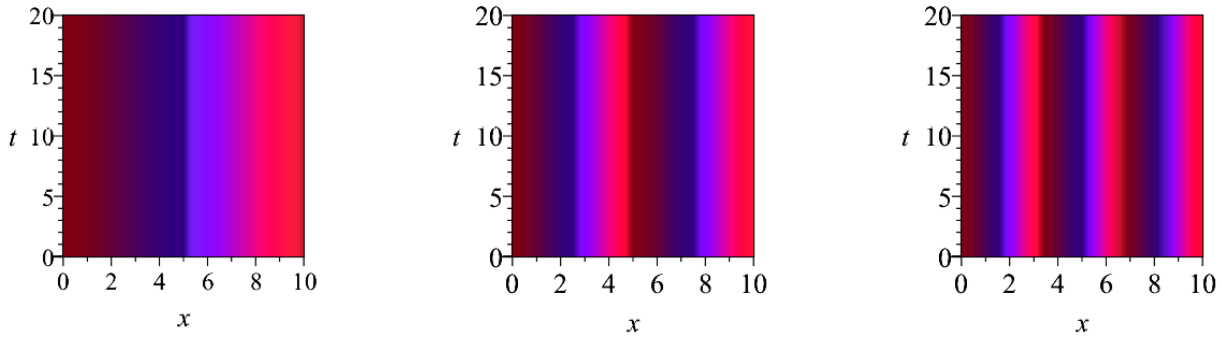

(a) $n = 1$ (b) $n = 2$ (c) $n = 3$

Figure 4.1: Contour plots of stationary pulse solutions with $\mathbf{D}_n$-symmetry corresponding to various modes k_n with wave numbers $n = 1, 2, 3$ as described in Section 4.1.

corresponding eigenspaces are $\mathbf{v}_1$ and $\mathbf{v}_2$ where,

$$\mathbf{v}_1 = (a_1 + ib_1)\, f_1 + (a_2 + ib_2)\, f_2 + c_1 f_3 + c_2 f_4,$$
$$\mathbf{v}_2 = -\overline{(a_1 + ib_1)} f_1 + \overline{(a_2 + ib_2)} f_2 - c_1 f_3 + c_2 f_4,$$

with $\{a_k, b_k, c_k\} \in \mathbb{R}$ for $k = 1, 2$. Therefore, the eigenfunction is given as,

$$U(x,t) = z_1 e^{i\omega t} e^{ik_n x} \mathbf{v}_1 - z_2 e^{i\omega t} e^{-ik_n x} \overline{\mathbf{v}}_2 + c.c. \tag{4.3.5}$$

We also recall Eq. (3.3.14) from Chapter 3.3

$$h_1^n = e^{ik_n x} \mathbf{v}_1, \qquad\qquad h_2^n = -e^{-ik_n x} \overline{\mathbf{v}}_2,$$

to obtain the eigenfunction corresponding to purely imaginary eigenvalues of the form

$$U(x,t) = z_1 e^{i\omega t} h_1^n + z_2 e^{i\omega t} h_2^n + \mathbf{c.c.}. \tag{4.3.6}$$

Since $f_1 = (1, 1, 0, 0)^T$, $f_2 = (1, -1, 0, 0)^T$, $f_3 = (0, 0, 1, 1)^T$, $f_4 = (0, 0, 1, -1)^T$, we can

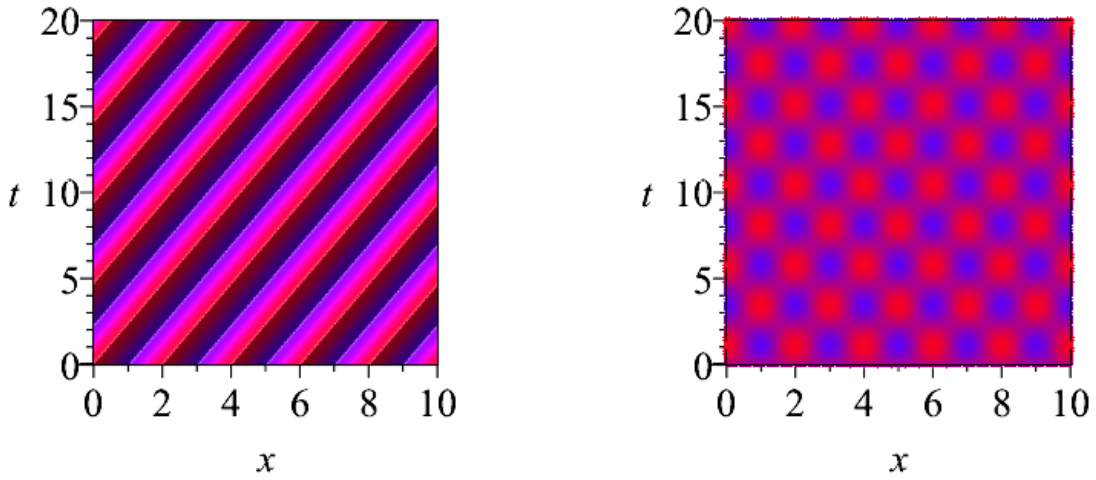

(a) R.W. with $n = 5$ (b) S.W. with $n = 5$

Figure 4.2: Contour plots of the total densities of the rotating and standing wave solutions with wave number $n = 5$ and $\widetilde{\mathbf{SO(2)}}$-symmetry and SW-symmetry, respectively, as described in Section 4.2.

write $\mathbf{v}_1$ and $\mathbf{v}_2$ as follows

$$\mathbf{v}_1 = \begin{bmatrix} (a_1 + a_2) + i(b_1 + b_2) \\ (a_1 - a_2) + i(b_1 - b_2) \\ c_1 + c_2 \\ c_1 - c_2 \end{bmatrix}, \qquad \mathbf{v}_2 = \begin{bmatrix} (-a_1 + a_2) + i(b_1 - b_2) \\ -(a_1 + a_2) + i(b_1 + b_2) \\ -c_1 + c_2 \\ -c_1 - c_2 \end{bmatrix} \tag{4.3.7}$$

and then expand (4.3.6) as

$$U(x,t) = e^{i\omega t} \begin{bmatrix} z_1 e^{ik_n x}\left[(a_1 + a_2) + i(b_1 + b_2)\right] - z_2 e^{-ik_n x}\left[(-a_1 + a_2) - i(b_1 - b_2)\right] \\ z_1 e^{ik_n x}\left[(a_1 - a_2) + i(b_1 - b_2)\right] + z_2 e^{-ik_n x}\left[(a_1 + a_2) + i(b_1 + b_2)\right] \\ z_1 e^{ik_n x}(c_1 + c_2) - z_2 e^{-ik_n x}(-c_1 + c_2) \\ z_1 e^{ik_n x}(c_1 - c_2) + z_2 e^{-ik_n x}(c_1 + c_2) \end{bmatrix}. \tag{4.3.8}$$

The total density $w(x,t)$ for (4.3.8) is given as

$$w(x,t) = 2e^{i\omega t}\left(a_1 + c_1 + ib_1\right)\left(z_1 e^{ik_n x} + z_2 e^{-ik_n x}\right) + \text{c.c.}. \tag{4.3.9}$$

Isotropy Subgroup	Orbit Representative	Type
$\mathbf{O(2)} \times \mathbf{S^1}$	$(0,0)$	Homogeneous Steady-State
$\widetilde{\mathbf{SO(2)}}$	$(b,0)$	Rotating Wave
$\mathbb{Z}_2(\kappa) \times Z_{2n}\left(\frac{L}{2n}, \pi\right)$	(b,b)	Standing Wave

Table 4.1: Isotropy subgroups, orbit representatives and type of primary bifurcating solutions on the center manifold as described in [19].

Isotropy Subgroup	$U(x,t)$	$w(x,t)$	Solution Type
$\mathbf{D}_n$	$\text{Re}\left(z_0 e^{ik_n x}\right)$	$4\text{Re}(z_0 e^{ik_n x})$	S.P.
$\widetilde{\mathbf{SO(2)}}$	$be^{i\omega t}h_1^n + c.c.$	$2be^{i\omega t}e^{ik_n x}\left(a_1 + c_1 + ib_1\right) + c.c.$	R.W.
$\mathbb{Z}_2(\kappa) \times Z_{2n}\left(\frac{L}{2n}, \pi\right)$	$be^{i\omega t}(h_1^n + h_2^n) + c.c.$	$4ibe^{i\omega t}\cos(k_n x)\left(a_1 + c_1 + ib_1\right) + c.c.$	S.W.

Table 4.2: Summary of eigenfunctions and the corresponding total densities of the S.P., R.W and S.W. solutions. We note that since we are denoting 2π as the period for these periodic solutions, thus $\pi \in \mathbf{S}^1$ denotes a temporal shift of half of a period.

Using the following orbit representatives from Table 4.1 we obtain the linear solutions for the primary bifurcating solution branches for the rotating wave

$$U(x,t) = be^{i\omega t}h_1^n + c.c., \tag{4.3.10}$$

with a total density of

$$w(x,t) = 2be^{i\omega t}e^{ik_n x}\left(a_1 + c_1 + ib_1\right) + c.c., \tag{4.3.11}$$

and the standing wave;

$$U(x,t) = be^{i\omega t}(h_1^n + h_2^n) + c.c., \tag{4.3.12}$$

with a total density of

$$w(x,t) = 4ibe^{i\omega t}\cos(k_n x)\,(a_1 + c_1 + ib_1) + c.c.. \tag{4.3.13}$$

We note that, the stationary pulse modes displayed by Figs. (4.1a – 4.1c) and the rotating and standing wave modes displayed by Figs. (4.2a, 4.2b) corresponding to the eigenfunctions from Table 4.2 are dominant patterns that occur near bifurcation.

4.4 Liapunov-Schmidt Reduction: A Generic Description

One of the main goals of this thesis is to describe the solution near the homogeneous steady-state solutions (2.3.2). In this section we give a generic description of the Liapunov-Schmidt reduction (LSR) as described by Golubitsky and Schaeffer [17]. After showing the existence of both zero and purely imaginary eigenvalues for the linearized system (3.2.9) in Section 3.3 the LSR allows us to put the solutions of the full system (2.1.1) locally into a one-to-one correspondence with the solutions of a finite dimensional system of Eqs. [17]. We start this discussion with the generic system of equations

$$\Phi\,(y,\lambda) = 0 \tag{4.4.1}$$

where $\Phi : \mathcal{X} \times \mathbb{R}^k \to \mathcal{Y}$ is a smooth mapping with Banach spaces $\mathcal{X}$ and $\mathcal{Y}$. The unknown vector that is to be solved is denoted by y and the vector of parameters is denoted by $\lambda = (\lambda_1, \ldots, \lambda_k)$. Let L be the linearization of the full system (4.4.1) about the homogeneous steady-state solutions $(A_u/2, A_u/2, A_v/2, A_v/2)$ and L admits a zero eigenvalue with

ker $L \neq \{0\}$, the first step of the LSR is the decomposition of the spaces $\mathcal{X}$ and $\mathcal{Y}$ as follows

$$\mathcal{X} = \ker L \oplus M, \qquad \mathcal{Y} = N \oplus \text{range } L \tag{4.4.2}$$

where M and N are chosen such that these are vector space complements to $\ker L$ and range L, respectively. Next, let $P : \mathcal{Y} \to \text{range } L$ denote the projection of $\mathcal{Y}$ onto range L with $\ker P = N$ with a complementary projection $I - P : \mathcal{Y} \to N$. Notice that for some $u \in \mathcal{X}$ then

$$u = 0 \text{ iff } Pu = 0 \text{ and } (I - P)u = 0.$$

This trivial observation highlighted in [17] leads to the expansion of the full system as follows; $P\Phi(y, \alpha) = 0$ if and only if

$$\begin{aligned} &(a) \qquad P\Phi(y, \lambda) = 0 \\ &(b) \quad (I - P)\Phi(y, \lambda) = 0 \end{aligned} \tag{4.4.3}$$

where the aim is to solve (4.4.3) (a) and (b) separately. Suppose without loss of generality we rescale the homogenous steady-states such that near $(0, 0)$ we have

$$G(y, \lambda) := P\Phi(y, \lambda) = 0$$

then $dG(0, 0) = Pd\Phi(0, 0)$ and $\ker dG(0, 0) = \ker Pd\Phi(0, 0) = \{0\}$, thus $dG(0, 0)$ is invertible. Note $y \in \mathcal{X}$ can be written as

$$y = y_1 + y_2. \qquad y_1 \in \ker L, \ y_2 \in M, \tag{4.4.4}$$

which then implies

$$G(y, \alpha) = G(y_1, y_2, \lambda) = P\Phi(y_1 + y_2, \lambda). \tag{4.4.5}$$

Since $G(0,0,0) = 0$ and $\partial_{y_2} G(0,0,0)$ is invertible then by the Implicit function theorem [17], there exists a unique solution y_2 for Eq. (4.4.3 (a)) written as

$$y_2 = W(y_1, \lambda), \tag{4.4.6}$$

with $W : \tilde{N} \times \Lambda \in \ker L \times \mathbb{R} \to M$ satisfying

$$P\Phi\left(y_1 + W(y_1,\lambda), \lambda\right) \equiv 0, \quad W(0,0) = 0, \ \ \forall\, (y_1, \lambda) \in N \times \Lambda. \tag{4.4.7}$$

Next, we obtain the bifurcation equation by substituting W into (4.4.3 (b)), that is,

$$g(y_1, \lambda) := (I - P)\Phi\left(y_1 + W(y_1,\lambda), \lambda\right) = 0 \tag{4.4.8}$$

with $g : \ker L \times \mathbb{R} \to N$. Suppose that we consider writing $\ker L$ in terms of the basis vectors $\{e_1, \ldots, e_n\}$ (i.e., $\ker L = \operatorname{span}\{e_1, \ldots, e_n\}$) then it follows that $y_1 = x_1 e_1 + \cdots + x_n e_n$ and (4.4.8) can be written as

$$g\left(x_1 e_1 + \cdots + x_n e_n, \lambda\right) = (I - P)\Phi\left(x_1 e_1 + \cdots + x_n e_n + W\left(x_1 e_1 + \cdots + x_n e_n, \lambda\right), \lambda\right).$$

In this section, we see how the LSR is used so that we can put the solutions of the full system (4.4.1) into a one-to-one correspondence with the solutions of a finite dimensional system of equations (4.4.8). Performing the reduction for the full system (2.1.1) is outside of the scope of this Thesis (Chapter 5). However, from the discussions by Golubitsky et al. [19], the symmetry properties that (2.1.1) possesses allows us to obtain the reduced equation $g(x, \lambda)$ of (2.1.1) and use it for further analysis in the following sections.

4.5 General Form of $\mathbf{O(2)}$ and $\mathbf{O(2)} \times \mathbf{S^1}$-Equivariant Mappings

In this section we determine more complete information about the branches of solutions found previously from Theorems (4.1.2, 4.2.2) by analyzing the general form of $\mathbf{O(2)}$-equivariant and $\mathbf{O(2)} \times \mathbf{S^1}$-equivariant mappings. We start with the $\mathbf{O(2)}$-equivariant mappings, as shown in Section 4.4 that Equation (4.1.1) can be written in the following form

$$\frac{dx}{dt} + g(x, \lambda) = 0 \tag{4.5.1}$$

via the Liapunov-Schmidt reduction. Where $g : \mathbb{R}^n \times \mathbb{R} \to \mathbb{R}^n$ is an $\mathbf{O(2)}$-equivariant mapping, it follows from [19] that the presence of the $\mathbf{O(2)}$-symmetry implies the general form of g as follows:

$$g(z) = p\left(z\bar{z}\right) z. \tag{4.5.2}$$

Therefore, the steady-state solution of (4.1.1) satisfy

$$g\left(z, \lambda\right) = p\left(u, \lambda\right) z = 0 \tag{4.5.3}$$

where $u = z\bar{z}$ and p is some polynomial. We seek nontrivial solutions z to (4.5.3) or equivalently we aim to solve

$$p\left(u, \lambda\right) = 0.$$

We first perform a Taylor series expansion on the polynomial p and without loss of generality we translate the steady-state solution to $(0, 0)$, we then obtain the following expression:

$$p\left(u, \lambda\right) = p\left(0, 0\right) + p_u\left(0, 0\right) u + p_\lambda\left(0, 0\right) \lambda + \frac{1}{2} p_{uu}\left(0, 0\right) u^2 + \text{h.o.t} = 0. \tag{4.5.4}$$

We require $p(0,0) = 0$ so that we have an eigenvalue crossing condition and ignoring the higher order terms gives us the following expansion

$$p(u,\lambda) \approx p_u(0,0)\, u + p_\lambda(0,0)\, \lambda = 0. \tag{4.5.5}$$

At the linear level in u, the nontrivial solutions to (4.5.3) are as follows

$$|z| = \pm \left[-\frac{p_\lambda(0,0)}{p_u(0,0)} \lambda \right]^{1/2}. \tag{4.5.6}$$

Given the solutions (4.5.6), we now classify the branches of solutions that are obtained from Theorem (4.1.3) in terms of their criticality. The two cases below illustrate all of the possible scenarios for the solutions (4.5.6)

- **Case 1** $\left(\frac{p_\lambda(0,0)}{p_u(0,0)} < 0\right)$: This case requires $p_u(0,0)\, p_\lambda(0,0) < 0$ and $\lambda > 0$. Thus the $\mathbf{D}_n$ branches are *supercritical*.
- **Case 2** $\left(\frac{p_\lambda(0,0)}{p_u(0,0)} > 0\right)$: This case requires $p_u(0,0)\, p_\lambda(0,0) > 0$ and $\lambda < 0$. Thus the $\mathbf{D}_n$ branches are *subcritical*.

It was shown in [19]that there exists a LSR to an $\mathbf{O(2)} \times \mathbf{S^1}$-symmetric system that undergoes a Hopf bifurcation which admits the mapping

$$\tilde{g}(z_1, z_2, \lambda, \tau) = (p + iq) \begin{bmatrix} z_1 \\ \\ z_2 \end{bmatrix} + (r + is) \begin{bmatrix} z_1 \\ \\ -z_2 \end{bmatrix} \tag{4.5.7}$$

with $\tilde{g} : \mathbb{C}^2 \times \mathbb{R} \times \mathbb{R} \to \mathbb{C}^2$ and p, q, r, s are $\mathbf{O(2)} \times \mathbf{S^1}$ invariant polynomial. The LSR from [19] shows that

(a) $p(0) = 0$, $p_r(0) = 0$,

(b) $q(0) = 0$, $q_r(0) = -1$,

(c) $p_\lambda(0) \neq 0$ (eigenvalue crossing condition).

Then, [19] shows the leading terms of the branching equations for the rotating and standing waves are,

$$\lambda = \frac{-p_N(0) + r(0)}{p_\lambda(0)} a^2 + \cdots \tag{4.5.8a}$$

$$\lambda = \frac{-2p_N(0)}{p_\lambda(0)} a^2 + \cdots , \tag{4.5.8b}$$

respectively. Equations (4.5.8) determine the directions of branching of both rotating and standing waves depending on the values of $p_N(0)$ and $r(0)$ which can be obtained explicitly using LSR.

Chapter 5

Summary of Results and Future Work

It was shown by Buono and Eftimie [4] that the one-communication mechanism models (e.g., **M**1–**M**5) introduced by Eftimie et al. [11, 12] possess symmetry properties. In particular, Buono and Eftimie [4] proves the **O(2)**-equivariance of the models **M**1–**M**5. Being an extension of the model by Eftimie et al. [12], we show that the two-communication mechanism models introduced by Eftimie [10] also exhibit **O(2)**-symmetry. In Chapter 2.2, we describe the actions of the group **O(2)** on the system (2.1.1) and its solutions via the translation (2.2.2) and reflection (2.2.3) actions. This symmetry perspective allows us to determine various theoretical results that can be used to compare to numerical simulations for future studies. First, the **O(2)**-symmetry of the system enables the decomposition of the linear operator $\mathcal{L}$ into 4×4 matrices $\mathcal{L}_n$ using isotypic decomposition techniques. The bifurcation analysis begins with the computations of the critical eigenvalues of $\mathcal{L}_n$. In Chapter 3 we show the conditions for the parameters (q_a, q_r) that guarantees zero or purely imaginary eigenvalues. Figure 3.1 displays neutral stability curves for various values of n and $q_{al} = 0$ that correspond to the specific values of (q_a, q_r) such that zero eigenvalues (i.e., dashed curves) and purely imaginary eigenvalues (i.e., solid curves) are obtained, it also

shows the existence of codimension-two bifurcations at the intersections of any two curves.

The computation of the zero and purely imaginary eigenvalues, leads to the discussion of symmetry-breaking of the $\mathbf{O(2)}$-symmetric steady-state (2.3.2). In particular, the Equivariant Branching Lemma is applied at a steady-state bifurcation and we show the existence of stationary pulse solutions (Figure 4.1) with $\mathbf{D}_n$-symmetry emanating from (2.3.2). In the case where a Hopf bifurcation occurs, the Equivariant Hopf Theorem is applied to show that two types of periodic solutions emanate from (2.3.2): rotating waves (Figure 4.2a) and standing waves (Figure 4.2b) which exhibit $\widetilde{\mathbf{SO(2)}}$ and $\mathbb{Z}_2(\kappa) \times Z\left(\frac{L}{2n}, \pi\right)$ symmetries, respectively. After showing the existence of stationary pulse, rotating wave, and standing wave solutions, we calculate the eigenfunctions of the linearization at the homogeneous equilibrium (2.3.2). In Section 4.5, we determine the criticality of the bifurcating branches of solution by following the discussion in [19].

The results of this thesis are mainly theoretical, however, this opens several suggestions for future research. First, numerical simulations can be done to demonstrate the patterns from Section 4 predicted by the values of (q_a, q_r) via the neutral stability curves from Figure 3.1. As mentioned in Section 3.3, further study regarding the convergence or divergence of these neutral stability curves as $k_n \to \infty$ are required to obtain a region for asymptotic stability for large k_n values. We note that, in this thesis we only considered the repulsion and attraction terms (i.e., $q_{al} = 0$), however, there is evidence from [11, 12] of more complex patterns being obtained after the alignment term is incorporated to the simulations. It would be interesting to see the consequence of a nonzero q_{al} parameter value for this analysis and determine how the critical eigenvalue curves depend on q_{al}. We have also only considered the $\mathbf{M}3$–$\mathbf{M}4$ model, the same analysis can be performed to the other two-communication mechanism models from [10] and a comparison of the results (i.e., emanating branches of solutions at bifurcation) can be done. It is mentioned in Section 4.5 that the Liapunov-Schmidt reduction leads to the $\mathbf{O(2)}$-equivariant mapping (4.5.2) and (4.5.7). As mentioned in Section 4.4 the reduction itself is not performed

in this thesis and will be left for future studies from which the criticality of the bifurcating branches can be determined. Lastly, the evident existence of codimension-two bifurcations from Figure 3.1 can be further studied and discussed.

Bibliography

[1] birdinginformation.com. White Pelican, Accessed December 2016. URL `http://www.birdinginformation.com/birds/pelicans/white-pelican/`.

[2] P.C. Bressloff. Euclidean shift-twist symmetry in population models of self-aligning objects. *SIAM Journal on Applied Mathematics*, 64:1668–1690, 2004.

[3] Brian Dunbar. NASA - With an Eye on Locusts and Vegetation, Scientists Make a Good Tool Better, 2013. URL `https://www.nasa.gov/topics/earth/features/ndvi_locusts.html`.

[4] P-L Buono and R. Eftimie. Codimension-two bifurcations in animal aggregation models with symmetry. *SIAM Journal on Applied Dynamical Systems*, 13(4):1542–1582, 2014.

[5] P-L Buono and R. Eftimie. Symmetries and pattern formation in hyperbolic versus parabolic models for self-organised aggregation. *Journal of Mathematical Biology*, 71 (4):847–881, 2015.

[6] I. D. Couzin, J. Krause, R. James, Ruxton G., and N. Franks. Collective memory and spatial sorting in animal groups. *Journal of Theoretical Biology*, 218:1–11, 2002.

[7] C. Cutts and J. Speakman. Energy savings in formation flight of pink-footed geese. *Journal of Experimental Biology*, 189:251–261, 1994.

[8] J. A. Downing, Y. Rochon, M. Prusse, and Harvey H. Spatial aggregation, body size, and reproductive success in the freshwater mussel elliptio complanata. *Journal of the North American Benthological Society*, 12:148–156, 1993.

[9] R. Eftimie. Hyperbolic and kinetic models for self-organized biological aggregations and movement: a brief review. *Journal of Mathematical Biology*, 65(1):35–75, 2011.

[10] R. Eftimie. Simultaneous use of different communication mechanisms leads to spatial sorting and unexpected collective behaviours in animal groups. *Journal of Theoretical Biology*, 337:42–53, 2013.

[11] R. Eftimie, G. de Vries, and M. A. Lewis. Complex spatial group patterns result from different animal communication mechanisms. *Journal of Theoretical Biology*, 104(17): 6974–6979, 2007.

[12] R. Eftimie, G. de Vries, M. A. Lewis, and F. Lutcher. Modeling group formation and activity patterns in self-organizing collectives of individuals. *Journal of Mathematical Biology*, 69:1537–1565, 2007.

[13] R. Eftimie, G. de Vries, and M. A. Lewis. Weakly nonlinear analysis of a hyperbolic model for animal group formation. *Journal of Mathematical Biology*, 59(1):37–74, 2009.

[14] G. Flierl, Grünbaum D., S. Levin, and D. Olson. From individuals to aggregations] the interplay between behavior and physics. *Journal of Theoretical Biology*, 196(4): 397–454, 1999.

[15] H. I. Freedman and G. S. K. Wolkowicz. Predator-prey systems with group defence; the paradox of enrichment revisited. *Bulletin of Mathematical Biology*, 48:493–508, 1986.

[16] S. A. H Geritz and M. Gyllenberg. Group defense and the predator's functional response. *Journal of Mathematical Biology*, 66:705–717, 2013.

[17] M. Golubitsky and D. G. Schaeffer. *Singularities and Groups in Bifurcation Theory Volume I*, volume 51. Springer, New York, 1985.

[18] M. Golubitsky and I Stewart. *The Symmetry Perspective*, volume 200. Birkhäuser Verlag, Basel-Boston-Berlin, 2002.

[19] M. Golubitsky, I. Stewart, and D. G. Schaeffer. *Singularities and Groups in Bifurcation Theory Volume II*, volume 69. Springer, New York, 1988.

[20] S. Goss and J. Deneubourg. The self-organising clock pattern of *Messor Pergandei* (formicidae, myrmicinae). Insectes Sociaux, 36(4):339–347, 1989.

[21] B. Hall. *Lie Groups, Lie Algebras, and Representations: An Elementary Introduction*, volume 2. Springer, Cham-Heidelberg-New York-Dordrecht-London, 2003.

[22] J. P. Hallier and D. Gaertner. Drifting fish aggregation devices could act as an ecological trap for tropical tuna species. *Marine Ecology Progress Series*, 353:255–264, 2008.

[23] A. Huth and C. Wissel. The simulation of the movement of fish schools. *Journal of Theoretical Biology*, 156:365–385, 2002.

[24] C. Jerome, D. McInnes, and E. Adams. Group defense by colony-founding queens in the fire ant *Solenopsis invicta*. *Behavioral Ecology*, 9:301–308, 1998.

[25] M. Kovacic. On matrixfree pseudoarclength continuation methods applied to a nonlocal partial differential equation in 1+1d with pseudospectral timestepping. Master's thesis, University of Ontario Institute of Technology, 2013.

[26] R. A. Lukes, S. B. Chin, and S. J. Haake. The understanding and development of cycling aerodynamics. *Sports Engineering*, 8:59–74, 2005.

[27] A. Mogilner and L. Edelstein-Keshet. A non-local model for a swarm. *Journal of Mathematical Biology*, 38(6):534–537, 1999.

[28] OpenStax College. Large Fish School, 2011. URL `http://cnx.org/contents/Cp8sC4k_@5.1:ETfm5re9@3/Schooling-in-Fish`.

[29] K. Ouattara, A. Lemasson, and K. Zuberbühler. Anti-predator strategies of free-ranging campbell's monkeys. *Behaviour*, 146:1687–1708, 2009.

[30] J. K. Parrish and L. Edelstein-Keshet. Complexity, pattern, and evolutionary trade-offs in animal aggregation. *Science*, 284:99–101, 1999.

[31] T. J. Pedley. Collective behaviour of swimming micro-organisms. *Experimental Mechanics*, 50(9):1293–1301, 2010.

[32] B. Pfistner. Simulation of the dynamics of myxobacteria swarms based on a one-dimensional interaction model. *Journal of Biological Systems*, 3:579–588, 1995.

[33] D.A. Ritz. Is social aggregation in aquatic crustaceans a strategy to conserve energy? *Canadian Journal of Fisheries and Aquatic Sciences*, 57:59–67, 2000.

[34] P. Stapp, P. J. Perkins, and W. W. Mautz. Winter energy expenditure and the distribution of southern flying squirrels. *Canadian Journal of Zoology*, 69:2548–2555, 1991.

[35] The Ozone Hole. Swarm of krill, 1999. URL `http://www.theozonehole.com/krill.htm`.

[36] C .M. Topaz, A. L. Bertozzi, and M. A. Lewis. A nonlocal continuum model for biological aggregation. *Bulletin of Mathematical Biology*, 68:1601–1623, 2006.

[37] R. Vabøand L. Nøttestad. An individual based model of fish school reactions: predicting antipredator behaviour as observed in nature. *Fisheries Oceanography*, 6(3): 155–171, 1997.

[38] H. Weimerskirch, J. Martin, Y. Clerquin, P. Alexandre, and S. Jiraskova. Energy saving in flight formation. *Nature*, 413:697–8, 2001.

[39] Wikimeda Commons. Nunivak Musk Oxen in Defensive Formation, 2007. URL `http://animal.memozee.com/view.php?tid=2&did=3857&mode=full`.

[40] Wikimeda Commons. Tour of the Algarve 2012, 2012. URL `https://commons.wikimedia.org/wiki/File:Volta_ao_Algarve_2012_Team_Sky.jpg`.

[41] Wikimedia Commons: Doug Smith. Mollies Pack Wolves Baiting a Bison, 2011. URL `https://commons.wikimedia.org/wiki/File:Canis_lupus_pack_surrounding_Bison.jpg`.

[42] Wikimedia Commons: Primorsko. Starling murmuration Primorsko, 2016. URL `https://commons.wikimedia.org/wiki/File:Starling_murmuration_Primorsko2%_%E2%80%94_%D0%BA%D0%BE%D0%BF%D0%B8%D1%8F.jpg`.